Nitrogen Evolution, NO_X Formation and Reduction in Pressurized Oxy Coal Combustion

Zia ur Rahman[1], Xuebin Wang[1,*], Jiaye Zhang[1], Zhiwei Yang[2], Gaofeng Dai[1], Piyush Verma[2], Hrvoje Mikulcic[1,3], Milan Vujanovic[4], Houzhang Tan[1], Richard L. Axelbaum[2,*]

[1]MOE Key Laboratory of Thermo-Fluid Science and Engineering, Xi'an Jiaotong University, Xi'an, Shaanxi, 710049, China
e-mails: 4119999011@stu.xjtu.edu.cn, wxb005@mail.xjtu.edu.cn, daigaofn@qq.com,1695232523@qq.com, hzt@mail.xjtu.edu.cn

[2] Consortium for Clean Coal Utilization, Department of Energy, Environmental & Chemical Engineering, Washington University in St. Louis, St. Louis, MO, 63130, USA
e-mails: yang.zhiwei@wustl.edu, piyush.k.verma@wustl.edu, axelbaum@wustl.edu,

[3] Faculty of Mechanical Engineering and Naval Architecture
University of Zagreb, Zagreb, Croatia
e-mail: hrvoje.mikulcic@fsb.hr

[4] Faculty of Mechanical Engineering
University of Maribor, Maribor, Slovenia
e-mail: milan.vujanovic@fsb.hr

**Corresponding authors: wxb005@mail.xjtu.edu.cn; axelbaum@wustl.edu.*

Abstract: Oxy-combustion is one of the most prominent solutions for reducing CO_2 emissions from coal-fired power plants using carbon-capture-and-utilization technology. However, when compared to air combustion at atmospheric pressure, oxy-combustion is very expensive, owing to the significant efficiency penalties associated with air separation, flue gas recirculation (FGR), treatment, compression, and storage or transit of CO_2. In comparison, pressurized oxy-combustion (POC) is more efficient as it recovers a significant amount of heat energy from the flue gas moistures. Nevertheless, CO_2 derived from pressurized oxy coal combustion has impurities, e.g., acid gases (NO_X and SO_X) that can corrode the plant equipment, transport lines as well as deteriorating effect on the environment. Fortunately, in pressurized combustion systems, both NO_X and SO_X can be scrubbed by a single-column direct contact cooler (DCC), but this requires a minimum ratio of NO_X to SO_X at the inlet to be efficiently removed. Therefore, NOx is one of the important hindering parameters in commercializing the pressurized oxy-combustion. Although NOx evolution during oxy-coal combustion has been explored extensively at 1 atm, higher pressure studies are rare. Much still needs to be done to better understand the NO_X mechanism and the effects of different parameters on NO_X emissions under these conditions. This paper reviews the published literature on nitrogen evolution, NO_X formation and reduction in pressurized oxy-coal combustion. At higher pressures, the NO_X from fuel-bound nitrogen is generated through volatiles, tar and char, all of which are discussed. Where literature is not available, the effect of pressure on NOx evolution in different stages of coal combustion is predicted through CHEMKIN simulation. Homogeneous and heterogeneous pathways of NO_X formation and their destruction in pressurized oxy-coal combustion are evaluated. Additionally, the effect of pressure on a few mature and commercialized NOx abatement methods is explored. In the last, the future perspective and recommendation are given. This review will aid in the provision of basic knowledge about NOx evolution and control in pressurized fuel combustion, as well as the identification of new research areas to pursue.

Keywords: pressurized oxy-combustion, pressurized char-N, pressurized volatile-N, pressurized SNCR, pressurized reburning, direct contact column.

Highlights

- Volatile-N decreases with increasing pressure and increases with heating rate.
- Elevated pressure strengthens the gasification of CO_2 to CO.
- The de-NOx efficiency of SNCR and reburning enhanced at higher pressure.
- Conversion of NO to NO_2 is improved at elevated pressure.
- High pressure upgrades the heterogeneous NOx reduction with char.

Words count: 12131

Contents

Abbreviations			
POC:	pressurized oxy-combustion	NOx:	oxide of nitrogen
SOx:	oxide of sulphur	DCC:	direct contact cooler
FGR:	flue gas recirculation	CO_2:	carbon dioxide
GHG:	greenhouse gases	CCS:	carbon capture and storage
ASU:	air separation unit	EP:	electrostatic precipitator
FGD:	flue gas desulfurization	COE:	cost of electricity
ITEA:	instituto trentino edilizia abitativa	ENEL:	ente nazionale per l'energia elettrica
CANMET:	canada center for mineral and energy technology	HRSG:	heat recovery steam generator
BFW:	boiler feedwater	HP:	high pressure
IP:	intermediate pressure	LP:	low pressure
H:	heater	CCS:	carbon capture and storage
SPOC:	staged pressurized oxy-combustion	WUSTL:	Washington University in St. Louis
GPU:	gas processing unit	CT:	cooling tower
CW:	cooling water	Econ:	economizer
SC:	steam cycle	PFBC:	pressurized fluidized bed combustion
JSR:	jet stirrer reactor	ROP:	rate of production
SNCR:	selective non-catalytic reduction		

1. Introduction

Coal is one of the most ubiquitous energy resources around the world and is expected to be the main source for power generation in the foreseeable future [1-3]. In 2019, coal provided 27.2% of global primary energy needs and the largest share of the world's power generation at 38% [4]. Coal role is expected to remain stable for the next 20 years due to its low cost and easy availability [5]. However, as coal has become more widely used, environmental concerns about mining and combustion have grown in prominence [6]. Coal use is associated with a number of issues, including the emission of acid gases (NOx and SOx), volatile organic combustion matter (VOC), particulate matter, pollutant contamination in ground water, and so on. Furthermore, coal is highly intensive in carbon content; therefore coal combustion is regarded as a major source of greenhouse gas emissions [7]. CO_2 emissions from coal consumption alone reached 15 Gt in 2014, accounting for nearly half of total emissions [5]. As a result, coal use has been a focus of both energy and environmental reforms, gaining considerable attention.

Carbon capture and sequestration (CCS) is one of the most important methods for reducing greenhouse gas emissions [4]. Different methods of carbon capture were used in CCS technologies, including pre-combustion capture, post-combustion capture, and oxy-fuel combustion [8, 9]. Over the last two decades, oxy-fuel combustion, particularly oxy-fuel combustion at atmospheric pressure, has gotten a lot of attention [10-15]. In oxy-combustion process, the combustion takes place in the presence of pure oxygen and recycled flue gas, which is mostly made up of CO_2 with traces of water vapors and other contaminants. The RFG replaces the portion of N_2 that is normally present in the air environment and controls the temperature of the furnace chamber. The remaining flue gas is then treated to remove water vapors and pollutants before being stored or used for another purpose [16]. A simplified flow sheet of oxy-combustion is shown in Fig. 1 [8].

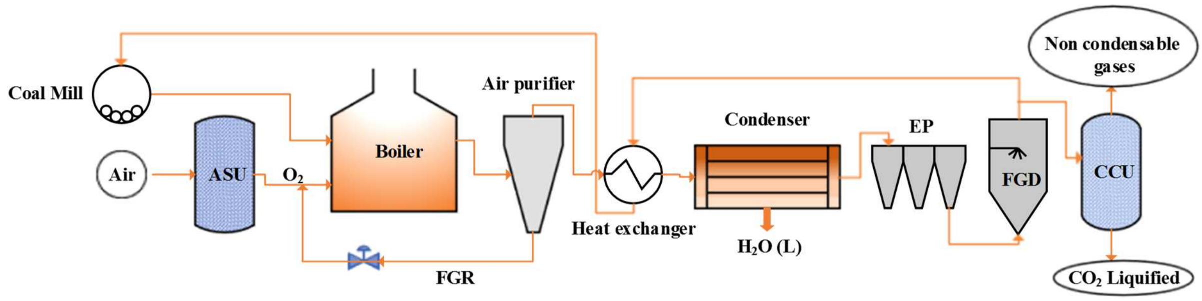

Fig.1. Basic flowchart of oxy-combustion (ASU: air separation unit, EP: electrostatic precipitator, FGD: flue gas desulfurization, CCU: carbon-dioxide compression unit) [8].

The high capital costs and low efficiencies of atmospheric oxy-combustion plants have limited efforts towards commercialization [17-19]. Recently, pressurized oxy-combustion (POC) has emerged as an attractive alternative due to its higher efficiency and smaller size. Several studies have assessed the technical and economic viability of this process [19-25], and research institutions have conducted experiments [26] and simulations of POC [27-29], and all concluded that the net efficiency of the POC process is significantly higher than the atmospheric oxy-combustion process. Not only does POC drastically reduce energy loss, but it also has a slew of other advantages, such as reducing boiler size, avoiding air leakage, and improving heat transfer [30, 31]. POC recovers more heat energy from the condensation of flue gas moisture because the dew point of water vapors is higher at elevated pressure than at atmospheric pressure. As a result, the POC system has a higher efficiency than the atmospheric oxy-combustion system. Furthermore, because the char combustion rate improves with increasing pressure, this technology (POC) can burn low-grade coal with high ash and/or water content, and much of the energy used to evaporate the moisture can be recovered [32]. The use of low-cost, low-quality coal results in significant cost-of-energy (COE) savings. In terms of COE, a 1% reduction in coal costs corresponds to a 0.5 percent increase in net efficiency [33]. ISOTHERM® is a patented pressurized coal combustion process developed by ITEA to burn inexpensive coal. ISOTHERM® boiler technology is a flameless boiler technology in which the combustion and heat transfer processes take place in separate boilers with the same pressure [34]. Such a practice helps prevent ash slagging or fouling problems resulting from the condensation of alkali compounds along the pipes and components downstream of the combustor. To illustrates these benefits, in 2006, ENEL started various experiments on the ITEA ISOTHERM® process [34] and has since carried out a number of tests at that 5 MW setup, operating at 4 bar [21, 22, 32, 33].

CANMET also conducted economical and technical analyses on a POC system based on the same technology (ISOTHERM®) [20]. Their approach resulted in higher net efficiency as well as lower capital and electricity costs in the POC system. The overall POC process using ISOTHERM® technology is summarized in Fig. 2, which consists of five major steps [35]: (1) cryogenic air separation; (2) pressurized coal combustion; (3) generation of steam; (4) power island; and (5) CO_2 treatment and compression unit. Coal is fed into a refractory-lined pressurized oxy-combustor, where flameless combustion takes place. There is no radiative heat transfer involved in this concept. The flue gas is routed to a convective heat recovery steam generator (HRSG). The coal is easily transported as coal water slurry to the pressurized burner and atomized by a small amount of medium pressure steam provided by the extracted turbine. The slurry water also helps to regulate the combustion temperature. To further control the combustor and HRSG inlet temperatures to around 1550 °C and 800 °C, a significant portion of the flue gas is recycled from the HRSG exit [36]. To prevent the condensation of acid gases, which would otherwise cause serious corrosion problems, the HRSG outlet temperature is kept at 330 °C, through the boiler feedwater (BFW) preheating temperature [25, 37, 38]. Finally, a two-stage compressor is used to compress flue gas at the CCS inlet.

Recently a novel staged, pressurized oxy-combustion (SPOC) has been introduced at Washington University in St. Louis (WUSTL) [39]. Fig. 3, depicts a simple SPOC process flow sheet. By designing the boiler in a series of stages, this method reduces the FGR by up to 30% and eliminates coal feeding in the form of slurry to regulate the combustion temperature [26]. Process analysis performed by WUSTL showed that reducing the FGR from 70% to 30% can lead to ~1.5 percentage point efficiency improvement, and the efficiency gain beyond 30% is marginal [40]. In this process, the four stages boilers are arranged in a series-parallel configuration. Coal and oxygen are supplied into these boilers in a consistent manner [26]. The recycled flue gas is fed into the first stage boiler to dilute oxygen and regulate the boiler temperature. Then, additional oxygen is mixed with a portion of the flue gas from the first boiler to the second stage boiler to keep the combustion temperature within the limit. The remaining first boiler flue gas is discharged downstream. The remaining two boilers are then treated in the same manner. Flue gas sent to the second, third, and fourth stages is nearly equal to that recycled to the first. Thus, all boilers operate in similar conditions. After further removing heat and ash with a high-temperature heat recovery unit and a particulate filter, the flue gas is passed through a DCC, which removes SOx and NOx while recovering the latent heat of the moisture in the flue gas. Due to the significantly lower FGR, the SPOC process has higher efficiency, reduced combustion-related equipment sizes, and also lower parasitic pumping loads [27, 28, 37, 39]. Furthermore, staging enhances plant operational flexibility by allowing one or more stages to be turned off while the others continue to operate at full capacity, resulting in efficient plant operation at low loads during the maintenance shutdown [26][26]. Staging and pressurization also enable a modular boiler design, potentially lowering construction costs and allowing for faster plant assembly [27].

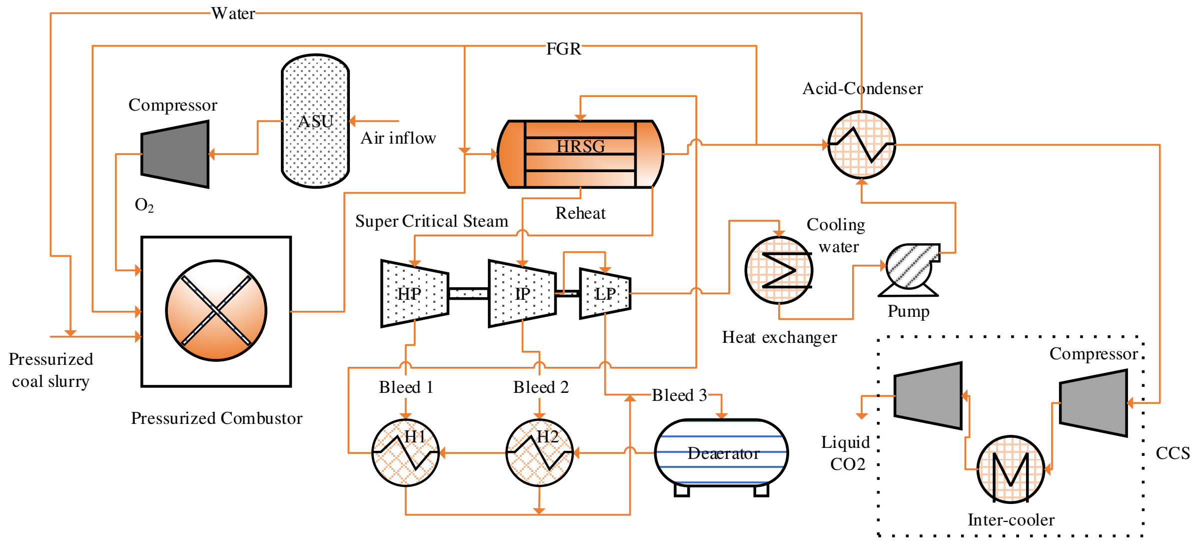

Fig. 2. Overall process diagram for the POC power cycle using ISOTHERM® technology, (ASU; air separation unit, HP; high pressure, IP; intermediate pressure, LP; low pressure, HRSG; heat recovery steam generator, H; heater, CCS; carbon capture and storage, FGR; flue gas recirculation.

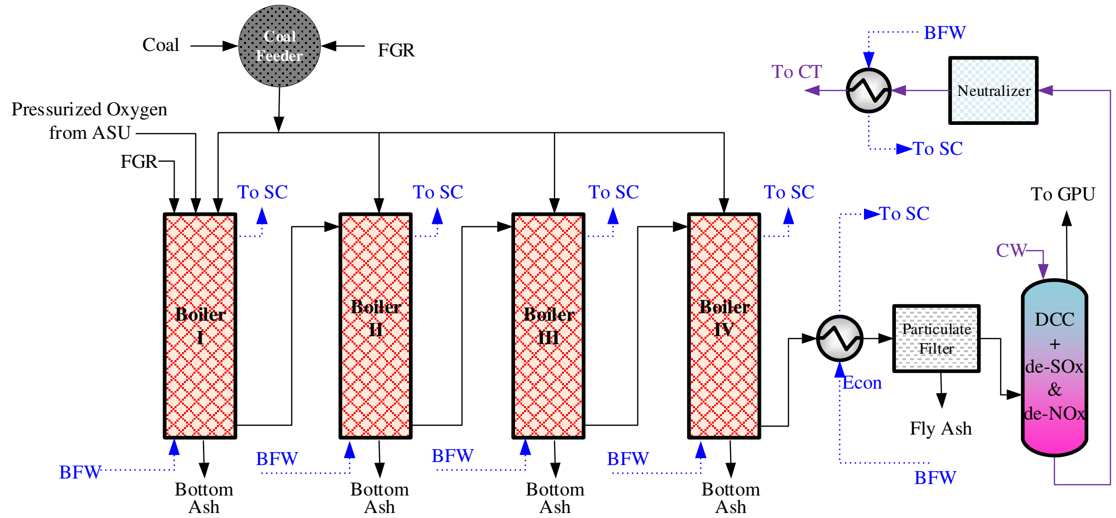

LEGEND				
ASU: Air Separation Unit	**BFW: Boiler Feed Water**	**GPU: Gas Processing Unit**	**CT: Cooling Tower**	**CW: Cooling Water**
DCC: Direct Contact Cooler	**Econ: Economizer**	**SC: Steam Cycle**	**FGR: Flue Gas Recirculation**	

Fig. 3. Schematic flow sheet of SPOC process [26, 39].

One of the main challenges for pressurizing oxy-combustion is to control the acid gases NO_X and SO_X after combustion, as they can lead to corrosion of plant equipment, transport lines as well as have worst effects on the environment. In pulverized coal boilers, the fuel-NOx mechanism produces 70 to 80 percent of NOx from fuel-bound nitrogen species (Fuel-N), and the remaining NOx is formed from atmospheric nitrogen (N_2) via the thermal-NOx mechanism (5-25%), and the prompt-NOx mechanism (less than 5%) [41]. The reactions involved in thermal NOx are N_2+O=NO+N, N+O_2=NO+O, N+OH=NO+H [42, 43]. The formation of thermal NOx is usually insignificant at temperatures lower than 1800 K. Prompt NOx is produced as a result of the reaction between the hydrocarbon radicals and molecular nitrogen according to the reaction $CH + N_2 \leftrightarrow NCN + H$ [42, 44, 45]. The Prompt NOx mechanism, on the other hand, has a very short lifetime of only a few microseconds, has little temperature dependence, and is more active in fuel-rich conditions. NO_X formed through the fuel-N mechanism accounts for about 200-800 ppm, while that produced through the other mechanisms is less than 50 ppm [46]. The oxidation of gaseous phase volatile-N and heterogeneous phase char-N is the primary source of NOx from fuel-N [47]. A simplified sketch for NOx formation from fuel-N is given in Fig. 4, modified from [3, 13, 48-54]. The concentration of nitrogen distributed between char and volatiles is primarily depends upon the fuel type, temperature, and pressure. In devolatilization, the coal-N is first released as a heavy structured and aromatic compound called tar and a small amount of ammonia (NH_3). Then the tar-N subsequently converts into hydrogen cyanide (HCN) and other light gases at high temperature via secondary pyrolysis. Depending on the stoichiometry and fuel-N concentration, HCN and NH_3 are either transformed into NO or N_2. At high temperatures, residual char-N is heterogeneously converted to NO and N_2 or releases HCN as a light component [55]. According to Loffler et al. [56], HCN is primarily converted into N_2O, whereas NH_3 transforms either NO or N_2. NO may react with hydrocarbon radicals and be converted into cyanide or reduced into N_2 by surface reactions on char or soot.

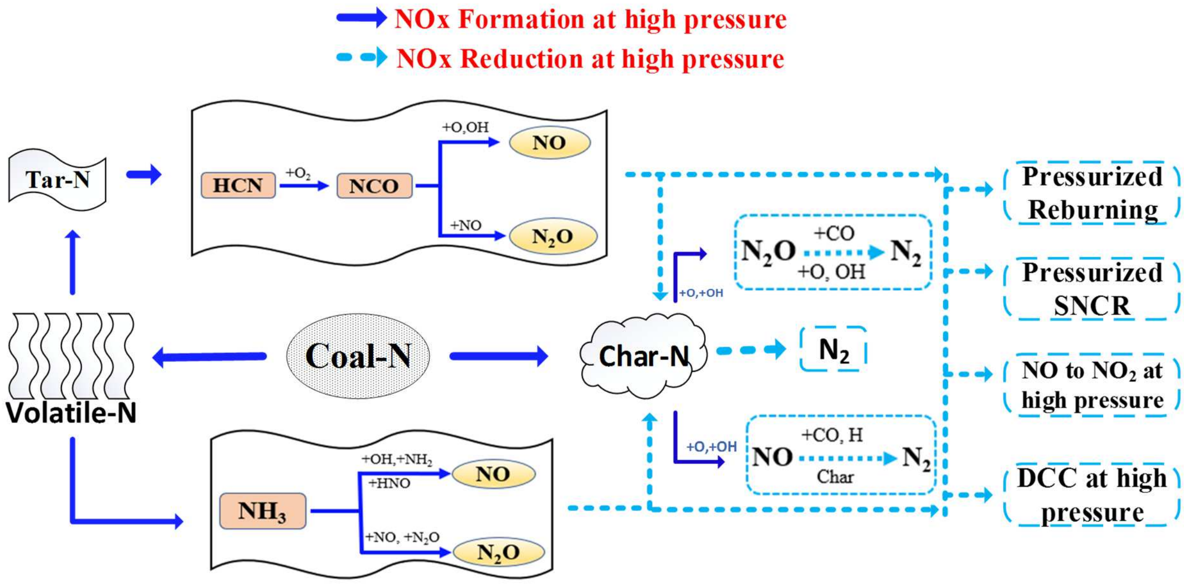

Fig. 4. Pathways of NOx formation and its reduction at high pressure from coal-N

There has already been a lot of research done on NOx evolution from oxy-coal combustion at 1 atm. In contrast, the evolution of NOx under the conditions of POC has received less attention. Aho et al. [57], analyzed the pressure effect on NOx formation and found that pressure increases have a major impact on NOx abatement, with NOx formation sharply declining as pressure rises. Croiset et al. [58], investigated the effect of pressure on NO formation and destruction during char combustion. They calculated the rate constant of the reaction $NO+C=1/2N_2+CO$ and found it to be pressure dependent. However, Tomeczec and Gill [59] investigated the rate constant of this reaction by following the same reaction conditions and realized that it is pressure independent. Lasek et al. [60], studied high pressure effect on NOx evolution in oxy-combustion of solid fuels and concluded that NOx is reduced at high pressure, which might be due to the enhancement of the char + NO reaction. Increased pressure, according to Nichols et al. [47], may improve the kinetic rates of NO reduction reactions and increase residence time, allowing more time for NOx reduction reactions. Another reason for NO abatement at high pressure is that the concentration of NO-promoting radicals may be suppressed at elevated pressure. The second point is based on a well-known explanation of nitrogen chemistry in flames [47]. The rate at which NO is reduced is commonly interpreted by:

$$\frac{d[NO]}{dt} = K[NO][NH_i] \qquad (1)$$

Substituting [NHi] with the mole fraction X_{NHi}, and multiplied by total concentration gives

$$\frac{d(\ln[NO])}{dt} = KX_{NHi}\left(\frac{P}{RT}\right) \qquad (2)$$

where R, P and T is the ideal gas constant, pressure, and temperature, respectively. According to Equation 2, by keeping the k and $X_{NHi,}$ constant, the reduction rate of the logarithm of NO concentration varies linearly to the pressure [47]. Calculations also show that as pressure rises, the concentrations of the O, OH, and H radicals falls, with HO_2 becoming the dominant radical at high pressure. These changes may be due to the three-body reaction $H + O_2 + M \leftrightarrow HO_2 + M$, which starts competing at 850°C with and ultimately dominate over the reaction $H + O_2 \leftrightarrow OH + O$ at elevated pressure. Because the O and OH radicles are important in the formation of NO, when they are reduced at high pressure, the formation of NO is reduced [47, 57, 61].

The NO_2 concentration is normally lower in flue gases produced at atmospheric pressure. Nonetheless, simulation analysis revealed that the NO_2 concentration could be prominent at higher pressures. Since, the concentration of HO_2 radical is more effective at a higher pressure, and NO reacts with HO_2 producing NO_2 [61, 62].

In summary, few studies have been reported on NOx formation and its reduction at high pressure, and there is still no clear consensus on the effects of pressure on NO_X evolution during oxy-coal combustion and following its reduction. Thus there exists a major knowledge gap on NOx evolution and its control under the POC conditions, and ultimately, this would negatively impact the technical design of NOx control techniques for future large-scale POC systems [63]. In that context, in this paper, we reviewed the published knowledge on nitrogen evolution, NOx formation, and reduction during pressurized oxy-coal combustion. The mechanisms of NOx formation in pressurized air and oxy-combustion have been discussed. Most importantly, at higher pressure, NOx from fuel-N are produced through the volatile, tar, and char, all of which are discussed. However, few studies are available on nitrogen evolution and the prediction of NOx formation and destruction at elevated pressure. In such cases, the effect of pressure on NOx evolution in different stages of coal combustion is predicted through the CHEMKIN simulation. Homogeneous and heterogeneous pathways of NOx formation and their reduction in pressurized oxy-coal combustion are discussed. Additionally, the effect of high pressure on a few of the mature and commercialized methods used for NOx abatement are evaluated. Based on the review literature, we identify research gaps in NOx evolution and control in POC that need to be addressed. This study will aid in a better knowledge of NOx chemistry and abatement approaches in pressurized oxy-coal combustion, as well as the identification of research directions for various NOx control methods.

The following is a breakdown of how the paper is structured; section 2 discusses the NOx emissions from pressurized air and oxy-combustion followed by the nitrogen evolution during the pressurized coal pyrolysis in N_2 and CO_2-rich atmosphere in section 3. Section 4 describes the volatile-N oxidation in pressurized oxy-combustion, while sections 5 and 6 delineate the oxidation of char-N and reduction of NO_X in pressurized oxy-combustion, respectively. Section 7 is the conclusion, and the last section is about the future perspectives and recommendations.

2. NOx emissions from pressurized air and oxy-combustion.

In this section, the NO_X evolution in pressurized combustion is reviewed. The review of NO_X emission is presented for pressurized air combustion in section 2.1 and pressurized oxy-combustion in section 2.2.

2.1. NOx emission from Pressurized air-coal combustion.

Pressurized combustion is recognized as a promising clean coal technology [64] for carbon capture and sequestration and abatement of acid gases NOx and SOx. NOx concentrations are normally reduced when the operating pressure is increased [65]. The pressure effect on the evolution of NO and N_2O in pressurized fluidized bed combustion (PFBC) for a Czech coal at temperatures between 845–855 °C is analyzed by Svoboda and Pohorely [66] and concluded that NO emission steadily decreases with increasing pressure. Other studies [67-70] have observed a similar effect of pressure on NO reduction, as shown in Fig. 5. The decrease of NO with pressure may be caused by the increase of O_2 partial pressure and the oxidation of NO to NO_2 [68]. A second reason is the interaction of char, CO, and NO at high pressure. High pressure retains the nitrogen-bearing species inside the pores of char particles for an extended time, allowing the nitrogen to be reduced to N_2. Lu et al.

[67], proposed that char combustion occurs earlier at high pressure compared to atmospheric pressure. Thus, the oxygen present in the air is used by volatile oxidation and char combustion. As a result, a large fraction of fuel-nitrogen converts to N_2 due to less oxygen availability in the furnace bed. Furthermore, the O_2 diffusion coefficient to the surface of char is reduced, i.e., in an air environment, the value decreases from 1.66 cm^2/sec to 0.46 cm^2/sec, while in an oxygen environment, the value decreases from 2.09 cm^2/sec to 0.52 cm^2/sec with increasing pressure from 0.1MPa to 0.4 Mpa, implying that the mobility of O_2 to the char becomes slower with increased pressure, resulting in low NOx formation from fuel-N [70, 71].

The mechanism for NO reduction has been explained by various researchers [72-76]. The partial pressures of NO and CO_2 increase with pressure. High CO_2 partial pressure leads to gasification reaction in the presence of char into CO through reaction R1 and decomposition/gassification of CO_2 into CO via R2;

$$CO_2 + C \leftrightarrow 2CO \qquad (R1)$$

and

$$2CO_2 \leftrightarrow 2CO + O_2 \qquad (R2)$$

The NO is homogeneously reduced by this CO via reaction R3 below [77]. Additionally, the residence time for NO in the pores of the char particles increases with increasing the pressure, resulting in a reduction of NO in the char particles via heterogeneous reaction R4 [63, 72, 77, 78]. In summary, the lower NO emissions with pressure are due to conditions favouring the homogeneous and heterogeneous reduction reactions shown in R3 and R4.

$$NO + CO \rightarrow \frac{1}{2}N_2 + CO_2 \qquad (R3)$$

$$NO + C \rightarrow \frac{1}{2}N_2 + CO \qquad (R4)$$

However, as shown in Fig. 6, the results of various studies on N_2O evolution under high pressure are contradictory. Unlike NO, no conclusive and satisfying explanation for the pressure effect on N_2O evolution has been published. Svoboda et al. [66] and Gong et al. [63], illustrated that N_2O increases slightly with pressure and argued that the increase of N_2O is a result of NOx reduction. However, Lu et al. [67] and Duan et al. [79], explored the pressure effect on N_2O and discovered a decreasing tendency, similar to NO. When the pressure was increased from 0.5 to 0.7 MPa, N_2O emissions were slightly reduced, as shown in Fig. 6. Duan et al. [79], concluded that both NO and N_2O are drastically reduced with pressure in both air and O_2/CO_2 environments. Roy et al. [80], investigated that N_2O formation is higher in an oxy-combustion environment than an air combustion environment. Hayhurst et al. [81], found that changing the combustion environment has little effect on N_2O emissions. Thus, there is no clear consensus on N_2O evolution in pressurized coal combustion. Therefore, more research is required to determine how N_2O is formed and reduced in pressurized air combustion.

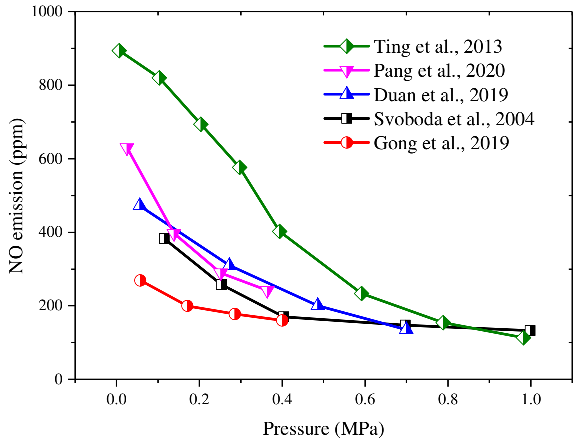

Fig. 5. Pressure effect on the conversion of fuel-N to NOx in PFBC [63, 66, 70, 79, 82].

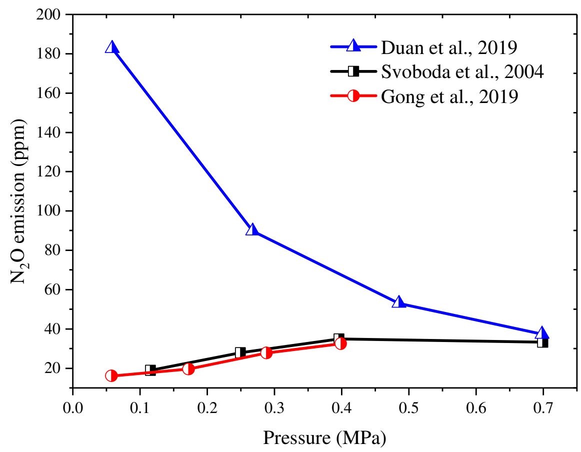

Fig. 6. Pressure effect on the emission of N_2O in the flue gases of PFBC [63, 66, 79].

2.2. NOx emission from Pressurized oxy-coal combustion.

POC is an emerging technology that can decrease energy demand compared to atmospheric oxy-combustion by recovering the latent heat of the flue gas moisture. Consequently, the net efficiency of the cycle is enhanced, and the size of the equipment is decreased. A number of studies in this area have been published [60, 74, 79, 83]. Lasek et al. [74], explored the formation of NO and N_2O under the high pressure in both oxy- and air-fired combustion and noted that increasing pressure helps suppress the production of NO and N_2O. However, as shown in Fig. 7, the impact of pressure is greater under air-fired than oxy-fired conditions. Lin et al. [84], observed that NO_X emission decreases significantly with pressure. They illustrated that the diffusion residence time for NO in char particles is extended with pressure, which reduces the NO concentration. According to Lin et al., pressure does not have a prominent impact on the formation of NO. But through reaction R4, pressure has a major influence on the NO reduction process due to the impact of the char surface. It is illustrated in Fig. 7, that, at high pressure, the formation of NOx (NO+N_2O) in air combustion is more significant than oxy-combustion, which may be due to the higher concentration of CO_2 in oxy-combustion. The CO_2 interacts with char to form CO through the Boudouard reaction ($CO_2 + C_s \leftrightarrow 2CO$). The resulting increase in CO concentration for oxy-combustion can facilitate the reverse reaction in R4 and, as a consequence, inhibit the reduction of NO.

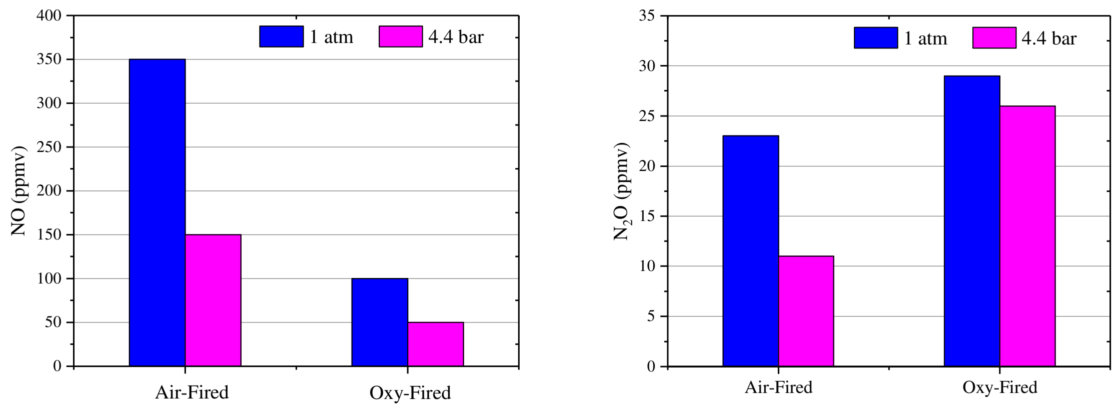

(a) (b)

Fig. 7. Pressure effect on (a) NO and (b) N_2O conversion during air- and oxy-combustion [74].

However, Duan et al. [79], reported a contrary result about NO_X emissions at high pressure from bituminous coal in air and oxy-combustion. NO, and N_2O are reduced considerably in both air and oxy atmospheres at high pressure, and the reduction of NO is more prominent in the lower pressure, i.e., ⩽0.3 MPa, as shown in Fig. 8. They found that the NO concentration is reduced more in oxy-combustion than air-fired combustion. The key explanation for this reduction is the high concentration of CO_2 in oxy-combustion, which promotes carbon gasification and facilitates the formation of CO through reactions R1 and

R2. The high CO concentration enhances the NO reduction by R3, resulting in a decrease in NO emissions.

Pressurized combustion could simultaneously minimize NO_X and CO emissions and increase combustion efficiency. Here, active radicals like O and OH serve a significant role in the formation of NOx at high pressure, and their concentrations can influence the NOx emissions. Aho et al. [57], confirmed this in a pressurized entrained-flow reactor and concluded that homogeneous NO formation reduces with an increase in pressure. They explained that as pressure increases, the three-body reaction $H + O_2(+M) \leftrightarrow HO_2(+M)$ competes with and ultimately dominates over $H + O_2 \leftrightarrow OH + O$ at 850 °C. This would lead to a drop in O and OH radicals, as well as NO.

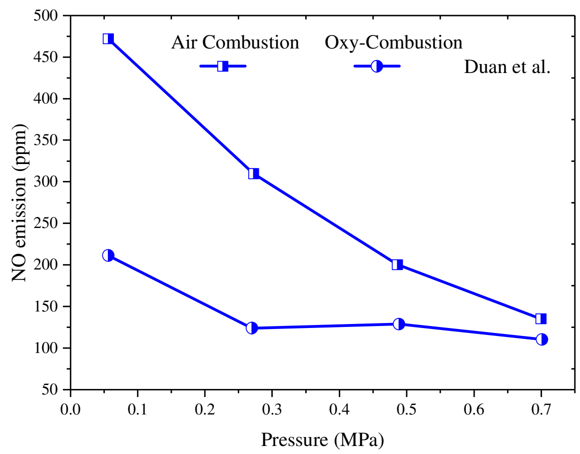

(a)

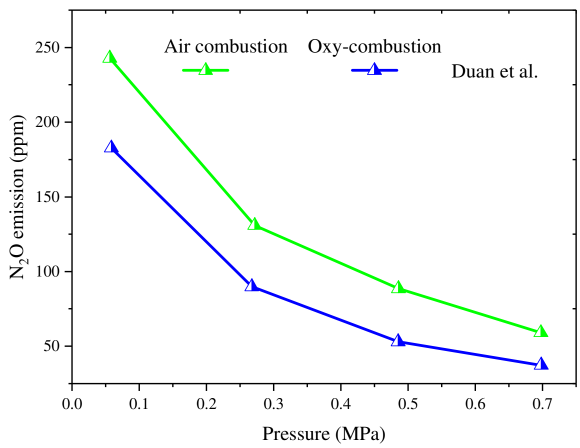

(b)

Fig. 8. Pressure effect on (a) NO_x emission and (b) N_2O emission in air-fired and oxy-combustion [79].

The NO formation from fuel-N during devolatilization step has been studied at different pressure by Veras et al. [85] and Aho et al. [57], and their results are shown together in Fig. 9. Veras et al. [85], found that the NO reduction is more pronounced when the pressure is elevated from 1 to 5 bar, however, the impact of pressure on NO reduction is minimal over the 5 bar. Similarly, Aho et al. [57], noticed that the NO concentration steadily decreased when the concentration of CO was less than 5000 ppm.

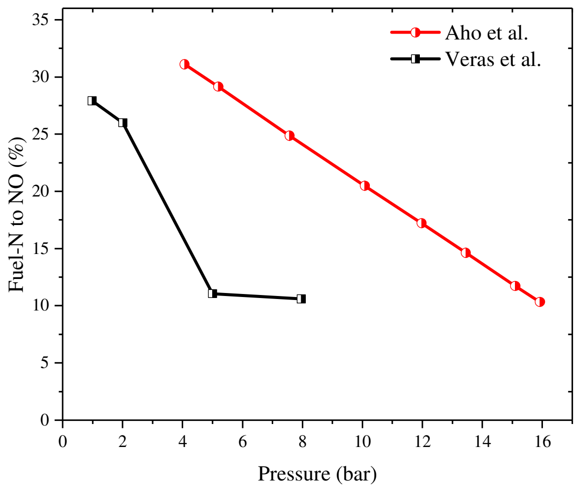

Fig. 9. Pressure effect on the conversion of fuel-N to NO. (a) Aho et al., [57], experimental conditions: T = 1000 K; $p(O_2)$ = 0.6 bar in a pressurized entrained flow reactor (b) Veras et al., [85], simulation conditions: T = 1350 K; O_2 = 10 wt%; particle dia 80 μm.

The evolution of N_2O under elevated pressure in an oxy environment has not been thoroughly researched, and the results are not coherent. Some researchers have found larger N_2O generation in pressurized combustion systems [62, 86], while others [57, 84] reported that there is no impact of pressure on the production of N_2O. Some have even observed the lower formation of N_2O at elevated pressures. This issue requires further study, especially for the case of oxy-combustion.

Overall, we come to the conclusion that pressure: 1) enhances the conversion of fuel-N to HCN and NH_3; 2) extends the NOx residence time within the char and promotes NO_X reduction by char; and 3) lowers the concentration of active radicles like O and OH, which leads to the suppression of NO formation. Thus, pressure influences NOx release in the O_2/CO_2 atmosphere through a combined effect of fuel-N oxidation and NOx reduction. The decrease in NO_X at higher pressure is due to the more significant influence of pressure on reducing NO_X than formation.

3. Nitrogen evolution during pressurized coal pyrolysis in inertial and CO_2-rich atmosphere.

The details of coal pyrolysis, aside from the volatile yield, are said to be of secondary importance to combustion. The reasoning is that pyrolysis happens quickly, whilst the char oxidation takes a long time, and thus the latter is in charge of the entire process. However, a closer examination reveals that pyrolytic processes, which typically precede thermal conversion processes (gasification and combustion), assert their impact over the entire solid-particle combustion process, from feeding to burnout [87]. Usually, coal-N is distributed into volatile-N and char-N mainly during the first step of pyrolysis. In the devolatilization step, the coal-N is first released within a heavy structured and aromatic compound called tar. The tar-N subsequently converts into HCN and other light gases at high temperatures via secondary pyrolysis.

3.1. Overall distribution of volatile, tar, and char-nitrogen

Detailed information on the formation mechanisms of NOx is required in order to develop methods for controlling and reducing NO_X during coal combustion. Only a few studies have been published on the influence of pressure on nitrogen evolution between volatiles and char [64]. However, because the mechanism for NOx formation from volatile-N and char-N are different, so this distribution is important to be explored. In addition, NOx control and reduction strategies rely mainly on the distribution of nitrogen between volatile and residual carbon [88]. The overall distribution of volatile, tar and char nitrogen is reviewed below.

3.2. Volatile-N

The coal fractionation into volatiles and char is important because volatiles are transformed into products on a smaller time frame than char. Devolatilization varies greatly, even within samples of the same type or rank of coal [89]. Therefore, information on devolatilization at high pressure is essential to understand the mechanism of pollutant formation and then devise an optimum control technique for the overall emissions in such systems [88]. During devolatilization, coal-N is transformed into volatile-N and char-N. NH_3, HCN, NO, N_2O and N_2 are the dominant nitrogenous gaseous products from devolatilization and combustion. These gases can be formed in a variety of ways. NO, N_2O and N_2 can be either produced from the homogeneous oxidation of NH_3 and HCN or from heterogeneous catalytic oxidation over char [64]. The trend for volatile release with pressure is shown in Fig. 10. Jenson et al. [64], illustrated that the volatile yield for Kiveton Park coal in a pressurized thermogravimetric analyzer decreases linearly as pressure increases. Similarly, Megaritis et al. [90] noted that the volatile yield from the pyrolysis of Daw Mill coal at 1000°C in a fluidized bed reactor decreases with pressure. The overall decrease in volatile release with pressure during pyrolysis can be understood in terms of physical suppression of devolatilization due to an increase in flow resistance with pressure. In addition, the volatilization process itself may be suppressed with pressure. Moreover, the decline in volatile yield with pressure agrees with the other investigations [83, 85, 88, 90, 91].

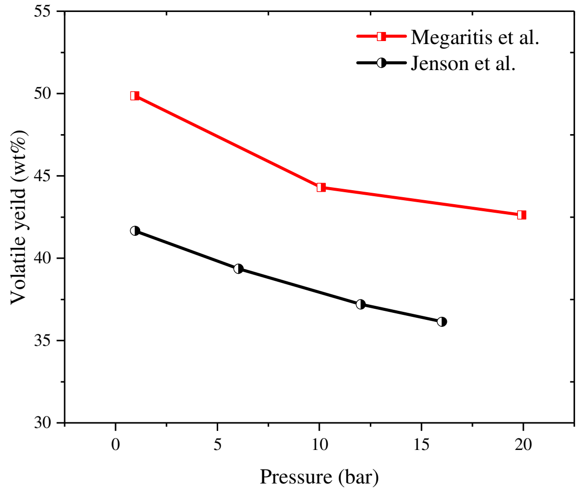

Fig. 10. Effect of pressure on volatile yield: (a) Jenson et al. [64], experimental conditions: T = 1173K; t(s) = 120 sec; Kiveton park coal; particle size range is 0.8-0.9 mm; facility used is pressurized thermogravimetric analyzer [64] (b) Megaritis et al., [90], experimental conditions: T = 1000 ^{o}C; t(s) = 60 sec; Daw mill coal; facility used is fluidized bed reactor.

NO is primarily produced either from NH_3 and HCN or directly from char-N oxidation. Meanwhile, NH_3 and HCN are formed either directly from the devolatilization of coal-N or from the secondary reaction of tar-N. A comprehensive literature survey by Johnsson [92] has shown that NH_3 and HCN are the major nitrogenous gaseous products from the devolatilization of coal-N during the pyrolysis process. The nitrogen in low-quality coals like brown coals and lignite is believed to be contained mostly in amine functional groups, which are converted into NH_3 at lower temperatures. Duan et al. [50], identified three key N-compounds in high-rank coals: pyridine, pyrrole, and quaternary nitrogen groups. HCN is usually produced from the conversion of pyridines and pyrrole nitrogen during pyrolysis at high temperatures. NH_3 is formed from two sources, one is from quaternary nitrogen decomposition, and the second is from tar-N and char-N secondary reactions. The development of NH_3 and HCN is further affected by the presence of CO_2. At lower temperatures, CO_2 is adsorbed on the surface of the coal matrix, blocking the contact of the H radical with the N site on the coal, while at higher temperatures, the coal matrix is exposed to reactive radicals from the gasification reactions [50]. Duan et al. [31], conducted experiments with a lab-scale pressurized fluidized bed reactor (PFBR) to investigate the effect of CO_2 at high pressure on the major nitrogenous pyrolysis products from devolatilization, i.e., NH_3 and HCN. They evaluated the concentration of nitrogenous gases produced from coal pyrolysis in

N_2 and CO_2 atmospheres as a function of pressure at 850 °C. A comparison of the HCN concentration in N_2 and CO_2 atmospheres is illustrated in Fig. 11(a). The maximum concentration of HCN in the N_2 and CO_2 environments steadily increased as pressure rised from 0.1 to 0.7 MPa. The thermal stability of pyridines and pyrrole nitrogen is high [55], and even at 1000 °C, they are not fully decomposed. However, the C/CO_2 bond is very active at high pressure since the stable -CN bond splits. Then, at high pressure, the open -CN sites promote the generation of HCN with H-radicals. Hence, it means that at higher pressure the HCN formation is prominently enhanced in CO_2 environment than the N_2 environment [50].

Fig. 11(b), illustrates the NH_3 concentration with respect to pressure in N_2 and CO_2 atmospheres. As is clear from the figure, the concentration of NH_3 shows a slight increase with pressure. This small increase is due to the fact that quaternary nitrogen decomposes nearly completely at around 800 °C, so the pressure effect on quaternary nitrogen splitting is negligible at 850 °C. The small increase in NH_3 may be due to char-N hydrogenation with H-radicals. The thermal cracking of the volatile precursors is facilitated by the increased residence time of the volatile precursors within the char at higher pressures, which creates more H-radicals that can react with char-N to form NH_3 [93].

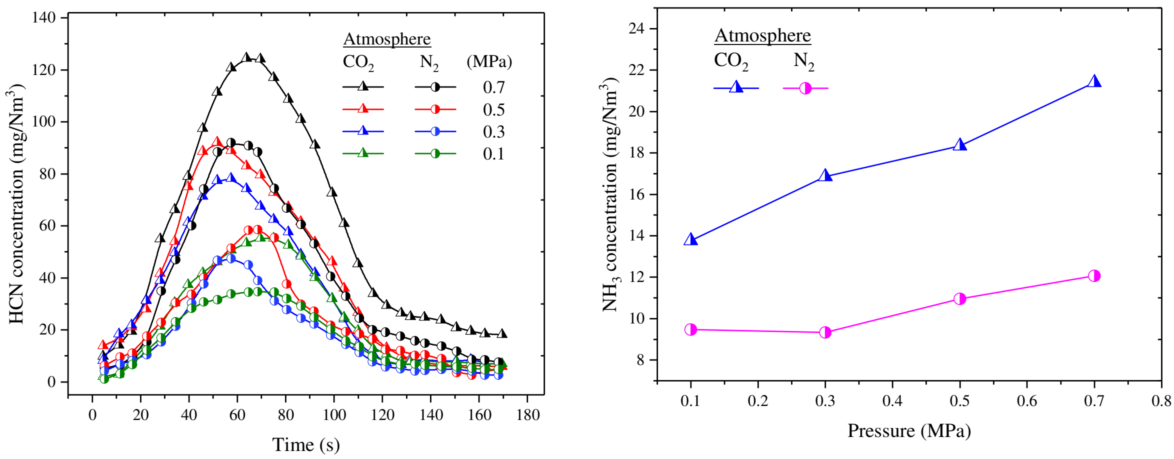

(a) (b)

Fig. 11. Effect of pressure and atmosphere on (a) HCN and (b) ammonia release during coal pyrolysis in a PFBR at 850 °C [31].

3.3. Tar-N

The distribution of nitrogen between char and volatiles depends primarily on the fuel type, temperature and pressure, as briefly described above. During devolatilization, the coal-N is first released with tar, a heavy structured and aromatic compound. The tar-N subsequently converts into HCN and other light gases at high temperatures via secondary pyrolysis [55]. High NH_3 concentrations have also been reported during secondary pyrolysis.

There are two types of volatile-N released during pyrolysis: fast volatile-N and slow volatile-N. Fast volatile-N is found in light tar compounds, which crack rapidly and produces NH_3 during secondary pyrolysis reactions. Whereas slow volatile-N (found in heavier tars) primarily produces HCN [62], which is then converted to either NO or N_2, depending on local stoichiometry and fuel-N concentration. Hämäläinen and Aho [62] have shown that the evaporation of the condensable phase formed at the initial stage of pyrolysis is hindered at high pressure and that diffusion through the particles is impeded. Thus, compared to atmospheric pressure, tar can experience more secondary exothermic reactions. These secondary reactions can be associated with either cracking that produces light hydrocarbons or re-polymerization that produces char:

$$Tar \rightarrow gas \qquad (R5)$$

$$Tar \rightarrow char \qquad (R6)$$

As a result, the time it takes for the primary product and char to interact with each other, increases with pressure, resulting in more char and gas and less tar. Studies have consistently shown a decrease in tar and an increase in volatiles with pressure [94, 95]. The work of Cai et al. [88], supported the previous studies by demonstrating that increasing the heating rate boosts the net transfer of nitrogen into tar while increasing the pressure hinders it, as shown in Fig. 12. Fig. 12 (a), illustrates that the difference between the yields of volatiles and tar is 20% at atmospheric pressure for high-rank U.S. coal Illinois No. 6. This difference increases to 30% at 7.0 MPa, suggesting that pressure contributes to the cracking of certain tar precursors into gaseous hydrocarbons. With increasing pressure, the decrease in total volatiles and tar yields is from 48 and 28% at 1atm pressure to 40 and 12% at 7.0 MPa for Illinois No. 6, and from 19 and 13% to 16 and 5% for Tilmanstone, respectively [88]. Moreover, the distribution of coal nitrogen between product phases as a function of pressure is shown in Fig. 12(b). This result shows that the N distribution with increasing pressure is strongly influenced by the type of coal. It can be observed in the figure that the distribution of volatile-N and tar-N decreases significantly as pressure increases for coal type Illinois No. 6, whereas pressure has little effect on the N-distribution in volatile and tar for coal type Tilmanstone.

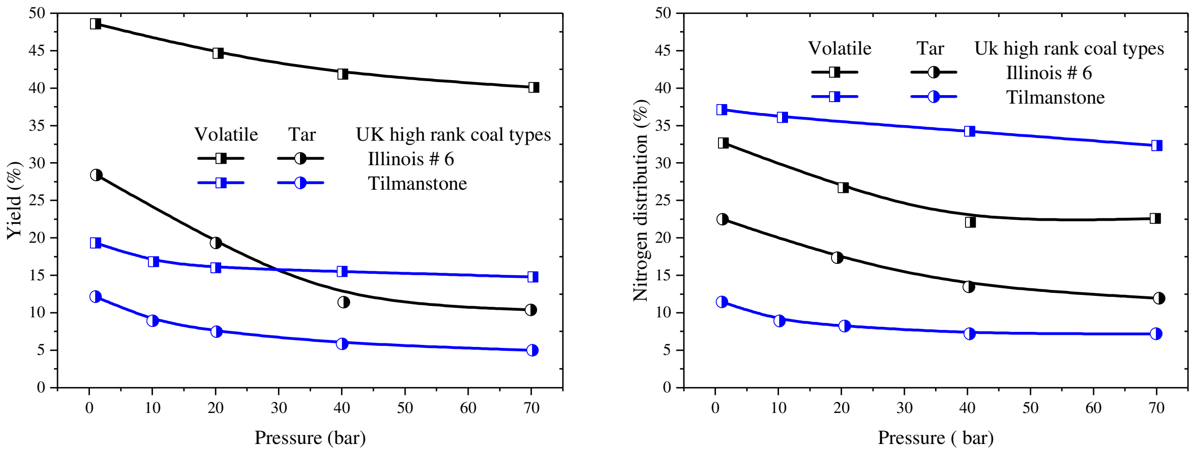

(a) (b)

Fig. 12. (a) Effect of pressure on (a) pyrolysis yield and (b) nitrogen distribution in pyrolysis yield for two types of high-rank UK coal at 700 °C and 10 s residence time [88].

3.4. Char-N

High-grade coal tars are more aromatic and stable at elevated temperatures than biomass and peat tars. They, therefore, appear to re-polymerize, generating char instead of cracking into simple gaseous molecules [62]. In the pyrolysis of Loy Yang (LY) brown coal at 700 °C, the yield of char, HCN, and NH_3 is plotted against pressure in Fig 13. The NH_3 yield increased significantly with pressure, but the HCN yield was only minimally affected. The near interactions between the char and the volatiles result in increased NH_3 and char yield during and after volatile release (precursors) [96]. Sathe et al. [97], conducted a similar study and found that increasing pressure raises radical concentrations in volatile precursors. Furthermore, the volatile precursors containing H-radicals have more time to react with the pyrolyzing coal-N to form NH_3 [93, 98, 99]. The increased retention time of such volatile precursors within the char would also increase free radical sites on the char surface [100]. These radical sites can increase soot formation during volatile-char interactions, resulting in the observed increase in char production with increased pressure during pyrolysis. The char proportion in Fig. 13, is confirmed by the work of Bayarsaikhan et al. [101], who found that increasing the pressure (1-12 atm) during the pyrolysis of Loy Yang brown coal at 900 °C increased the char production (on a carbon basis) in a similar nitrogen reactor.

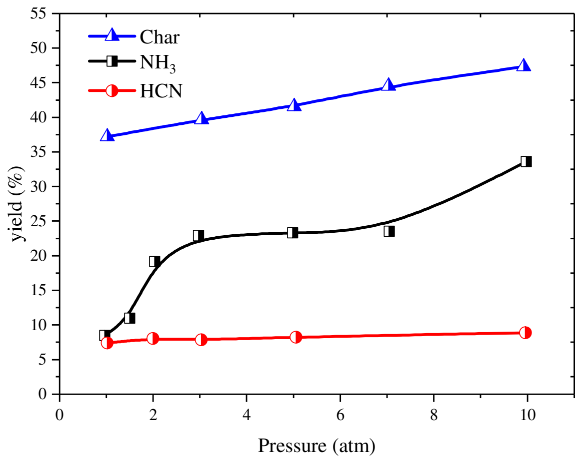

Fig. 13. Char, NH_3 and HCN yield with respect to pressure in the pyrolysis of LY brown coal at 700 °C [96].

Laughlin [102] investigated the effect of pressure (0.1-1.6 MPa) on the residual nitrogen in the char during the coal pyrolysis and concluded that the N/C ratio in the char was not affected by pressure, as shown in Fig 14(a). However, Maliutina [103] investigated the impact of pressure on nitrogen content in biomass char and found that the concentration of nitrogen in biomass char increased as pressure increased from 0.1 MPa to 1.5 MPa, but then decreased beyond 1.5 MPa, as illustrated in Fig 14(b). The explanation for this result is still uncertain, and there is no agreement on the effects of pressure on the distribution of char-N.

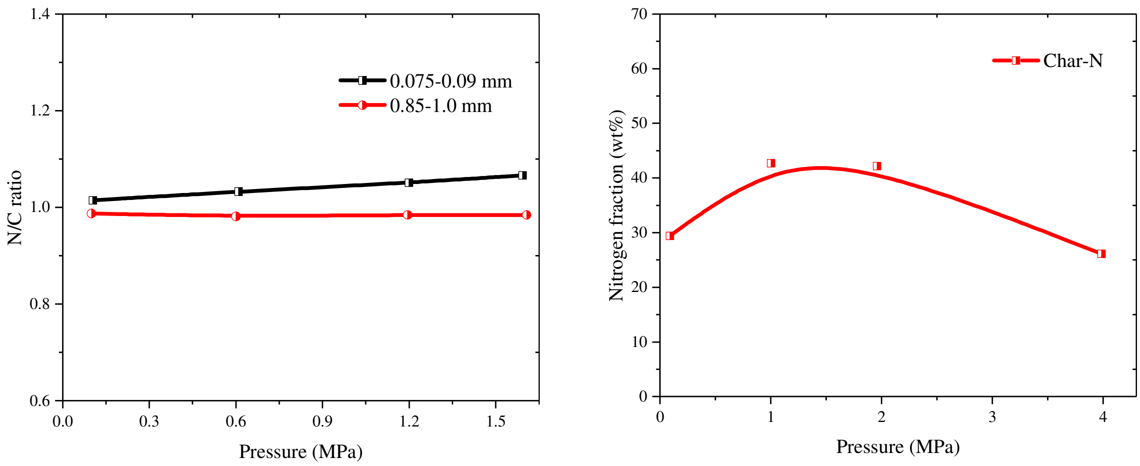

(a) (b)

Fig. 14. Pressure effect on char-N distribution; (a) coal pyrolysis (800-850°C), (b) biomass pyrolysis (600 °C).

4. Volatile-N oxidation in pressurized oxy-combustion.

In solid fuels combustion, NOx is primarily produced from the oxidation of volatile-N [104]. Thus, designing a low-NOx combustion system requires a comprehensive understanding of the volatile-N oxidation in pressurized oxy-combustion processes. The primary zone of a low NOx burner, where most of the fuel volatilization occurs, is typically operated at a fuel rich condition to reduce NOx formation from nitrogen-containing volatiles. As previously mentioned, the fuel-N is normally converted into HCN during the devolatilization stage of coal and high-grade fuel, whereas it is converted into NH_3 during the devolatilization stage of biomass or low-quality coal. HCN and NH_3 are either oxidized to NO or reduced to N_2 during the oxidation of volatile matter, depending on the reaction conditions. [42, 55].

4.1. HCN oxidation

The sources of cyanide formation during coal combustion are 1) the reaction of nitrogen species like NO or amine group compounds with the hydrocarbon radicals, 2) decomposition of hydrocarbon amines, and 3) the devolatilization of the organic bound nitrogen in coal [105-107]. The reaction chemistry of HCN — the most prominent cyanide species — at atmospheric pressure has been studied by several researchers in recent years [108-116]. However, there is a distinct lack of studies on HCN chemistry, including its oxidation mechanism at high pressures and temperatures. To predict the behaviour of HCN oxidation at high pressures, this work employs the Glaborg et al. [117], mechanism - a state-of-the-art reaction mechanism published in 2018. The comparison and validation of this mechanism can be seen in section 6.2. Chemkin simulations are used to understand the impact of high pressure (1-15 atm) and high temperature on HCN oxidation. Fig.15, display the predicted results of HCN oxidation at different pressure. We observe that with increasing pressure, the optimum temperature for HCN oxidation decreases, i.e., compared with 1 atm, at 15 atm, there is a 100 K decrease, from 1000 K to 900 K, in the oxidation starting point. This phenomenon could be the result of a reduction in ignition delay time at elevated pressures, as reported in studies for several different fuels [118-120]. Moreover, the Dikun Hong et al. [71], numerically investigated that CO_2 gasification is positively influenced at high pressure, producing an increased amount of CO and OH radicles via $CO_2+H \Leftrightarrow CO+OH$. The produced OH can improve HCN oxidation and CO can aid in NO reductions. Further, NO, and N_2O decrease while the intermediate HNCO and CO_2 increase respectively with the increase in pressure. The effect of pressure on the chemistry is significant upto10 atm with small changes above 10 atm. The main reaction pathways for HCN oxidation are shown in Fig. 16. The major and minor routes for HCN consumption are differentiated with different arrow thicknesses. HCN oxidation at atmospheric pressure is well established in the literature, but more work is required to understand the oxidation chemistry at high pressure.

From the rate of production (ROP) analysis, the most important reactions for HCN consumption at high pressure are;

$$HCN + OH \rightleftarrows CN + H_2O \qquad (R7)$$

$$HCN + OH \rightleftarrows HOCN + H \qquad (R8)$$

$$HCN + O \rightleftarrows NCO + H \qquad (R9)$$

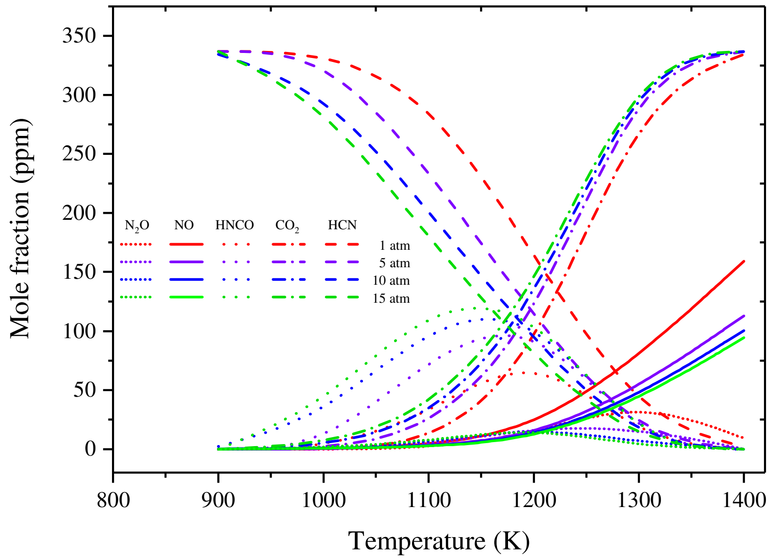

Fig. 15. Pressure effect on the HCN oxidation and their products respectively, Inlet condition: HCN = 337 ppm, H_2O = 3.1%, O_2 = 2.6%; reaction time = 0.149 s [110, 111].

$$OH + HCN \rightleftarrows HNCO + H \qquad (R10)$$

$$CN + HNCO \rightleftarrows HCN + NCO \qquad (R11)$$

$$HCN + O \rightleftarrows NH + CO \qquad (R12)$$

At high pressure, both NO and N_2O drop considerably with a small increase in CO_2 formation, as shown in Fig. 15. The main reaction involved in the consumption of NO and N_2O and the formation of CO_2 are;

$$NO + O + M \rightleftarrows NO_2 + M \qquad (R13)$$

$$NCO + NO \rightleftarrows N_2O + CO \qquad (R14)$$

$$NCO + NO \rightleftarrows N_2 + CO_2 \qquad (R15)$$

$$NH + NO \rightleftarrows N_2O + H \qquad (R16)$$

$$NH + NO \rightleftarrows N_2 + OH \qquad (R17)$$

$$N_2O + M \rightleftarrows N_2 + O + M \qquad (R18)$$

$$N_2O + CO \rightleftarrows N_2 + CO \qquad (R19)$$

$$N_2O + CO \rightleftarrows N_2 + CO_2 \qquad (R20)$$

$$O + CO(+M) \rightleftarrows CO_2(+M) \qquad (R21)$$

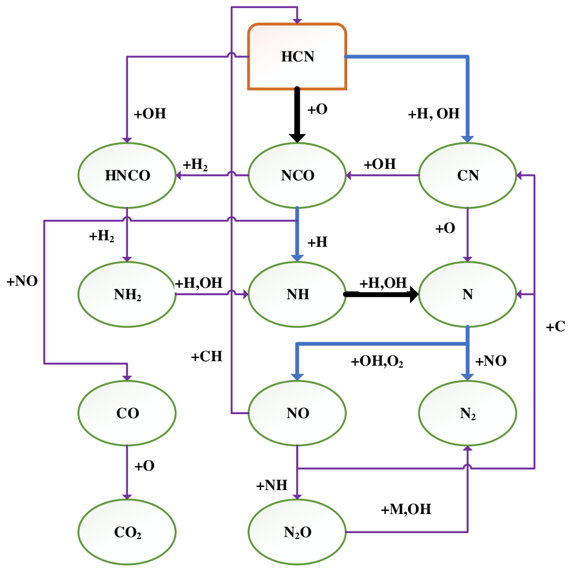

Fig. 16. Main reaction pathways of HCN oxidation at 15 atm.

4.2. NH₃ oxidation

Ammonia (NH_3) is formed during the early combustion and/or gasification process of coal [121] or biomass [122]. Ammonia has been used primarily to minimize NO_x in the SNCR process [123-126]. Ammonia has recently sparked interest as a possible carbon-free energy carrier [127]. Several studies on the modelling of ammonia chemistry in the combustion process have been published [42, 128-134]. It is one of the major sources of NO formation during the solid fuel oxidation phase [135]. Ammonia formed from the devolatilization of coal or biomass can be converted to NO or N_2 depending on the reaction conditions [42, 55, 135]. The pathway for NO or N_2 formation from the combustion of N-volatiles depends mainly on the structure of the amine radicals, such as NH_2, NH, and N [42, 55]. Since there are no studies available on NH_3 oxidation at high pressure and temperature, we employ the Glaborg et al. [117], mechanism in Chemkin simulation to understand the impact of high pressure and temperature on NH_3 oxidation. The results illustrated in Fig. 17, show that the optimum temperature window for NH_3 oxidation shifts significantly towards lower temperatures with increasing pressure. One possible explanation is that higher pressure increases the rate of the kinetic reactions responsible for ammonia consumption in the combustion processes such as $NH_3 + OH \rightleftarrows NH_2 + H_2O$, $NH_3(+M) \rightleftarrows NH_2 + H(+M)$, $NH_3 + H \rightleftarrows NH_2 + H_2$, and $NH_3 + O \rightleftarrows NH_2 + OH$. Due to this change in reaction rate, NH_3 starts oxidizing at lower temperatures, i.e., at 950 K compared to 1150 K at atmospheric pressure. Another possible hypothesis of this effect, supported by other works [118-120], stems from high pressure reducing the ignition delay time, which lowers the oxidation temperature. Furthermore, the concentration of NO decreases as pressure rises, signifying that higher pressure has a beneficial effect on NOx reduction efficiency. The most important reactions in the NO reduction are; $NH_2 + NO \rightleftarrows N_2 + H_2O$, $NH_2 + NO \rightleftarrows NNH + OH$, $NNH + NO \rightleftarrows N_2 + HNO$, $NO + H(+M) \rightleftarrows HNO(+M)$, $NO + HO_2 \rightleftarrows NO_2 + OH$, $NCO + NO \rightleftarrows N_2 + CO_2$, $NH + NO \rightleftarrows N_2O + OH$, $NH + NO \rightleftarrows N_2 + OH$, $NO + O(+M) \rightleftarrows NO_2(+M)$, $NO + OH(+M) \rightleftarrows HONO(+M)$, $N_2O(+M) \rightleftarrows N_2 + O(+M)$.

Similarly, the effect of high pressure on NH_3 oxidation and NO reduction were presented by Yu song et al., [136], but their analysis was conducted at intermediate temperature, i.e., 450 to 950 K. They concluded that at 30 bar NH_3 oxidation begins at 850-875 K and reduces down to 800 K at 100 bar. The products from NH_3 combustion mainly consisted of N_2 and N_2O with small amounts of NO and NO_2. The results suggest that that high pressure selectively suppresses the kinetics of NO_x formation reactions.

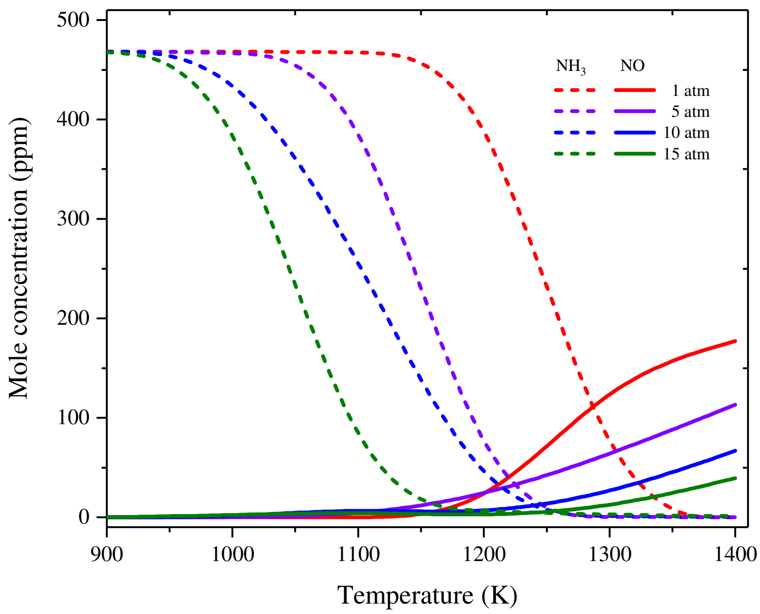

Fig. 17. Effect of different pressure on NH_3 oxidation and NO formation, initial condition; NH_4 = 468 ppm, CH_4= 2513 ppm, O_2=5040 ppm, residence time= 1.127 sec.

Fig. 18, shows the reaction pathways under the oxidizing conditions and pressure range of 30 to 100 bar. The thickness of the arrow separates the primary and secondary routes for ammonia use. The main route for ammonia consumption is $NH_3 + OH \rightleftarrows NH_2 + H_2$. At high pressure and low to moderate temperatures, the peroxide radical HO_2 is the main chain carrier under current conditions. However, some of the HO_2 is converted to OH via the fast steps R22 and R23,

$$NO + HO_2 \rightleftarrows NO_2 + OH \qquad (R22)$$

$$NH_2 + HO_2 \rightleftarrows H_2NO + OH \qquad (R23)$$

In addition, NH_2 reacts mainly with NO_2 via R24 and R25,

$$NH_2 + NO_2 \rightleftarrows N_2O + H_2O \qquad (R24)$$

$$NH_2 + NO_2 \rightleftarrows H_2NO + NO \qquad (R25)$$

NH_2 mainly converted to H_2NO, reacts with O_2, HO_2, and NO_2 via R26, R27, and R28, respectively; each of these reactions abstract one H atom from H_2NO to produce HNO, which is converted to NO by reaction with O_2 through R29.

$$H_2NO + O_2 \rightleftarrows HNO + HO_2 \qquad (R26)$$

$$H_2NO + HO_2 \rightleftarrows HNO + H_2O_2 \qquad (R27)$$

$$HNO + NO_2 \rightleftarrows HNO + HONO \qquad (R28)$$

$$HNO + O_2 \rightleftarrows NO + HO_2 \qquad (R29)$$

Finally, NO can react with either NH_2 or HO_2. The NH_2 + NO reaction produces N_2 either directly

$$NH_2 + NO \rightleftarrows N_2 + H_2O \qquad (R30)$$

or via

$$NH_2 + NO \rightleftarrows NNH + OH \qquad (R31)$$

this is accompanied by a rapid dissociation of NNH from the third body (+M),

$$NNH \overset{+M}{\rightleftarrows} N_2 + H \qquad (R32)$$

or

$$NNH + O_2 \rightleftarrows N_2 + HO_2 \qquad (R33)$$

In oxidizing condition, the reaction $NH_2 + NO_2 \rightleftarrows N_2O + H_2O$ is the key source of N_2O at both 30 bar and 100 bar. From sensitivity analysis, it was found that the most sensitive chain promoting reactions in ammonia combustion are $NH_2 + NO \rightleftarrows NNH + OH$, and $NH_2 + HO_2 \rightleftarrows H_2NO + OH$, supported by the formation of OH radicals, while the chain-terminating reactions are $NH_2 + NO \rightleftarrows N_2 + H_2O$ and $NH_2 + NO_2 \rightleftarrows N_2O + H_2O$. These reactions are based on the most recent work by Klipstein et al. [137] and Song et al. [136].

Duynslaegher et al. [138], investigated the influence of initial temperature and pressure on NO_x evolution from ammonia combustion in an internal combustion engine. They reported that NO evolution increased with an increase in temperature, mainly due to higher thermal NOx formation in the flame at high temperatures. Additionally, they found that even though an increase in the initial pressure does not significantly change the final flame temperature, the thermal NO formation decreased significantly with increasing pressure, as shown in Fig. 19. They conclude that temperature is not the only parameter to be considered for NO formation from the combustion of ammonia. A possible explanation for this phenomenon is that higher pressure suppresses the kinetics of NO formation reactions. However, to understand NO formation in ammonia flames under high pressure and temperature conditions, further analysis of such influences are required.

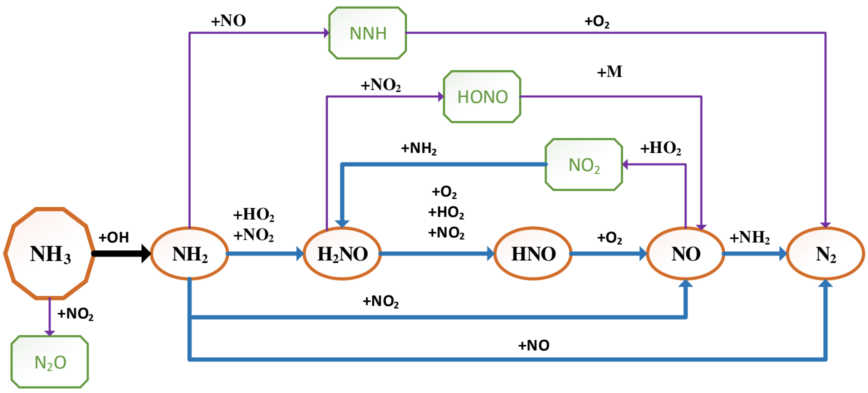

Fig. 18. NH_3 oxidation reaction path ways at the elevated pressure (30-100 bar).

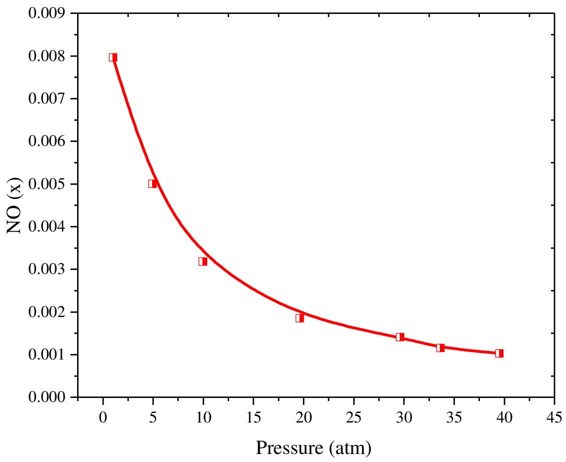

Fig. 19. Effect of different pressures on NO mole concentration in the flame [138].

5. Oxidation of char-N in pressurized combustion.

Lin et al. [84], analyzed the pressure effect on char particle combustion and the formation of NOx from char-N. They found that in a diffusion-limited high-temperature regime, the emission of NO_x dropped dramatically with rising pressure. Pressure impedes NOx diffusion from the char particle, causing the residence time of NOx to increase. Consequently, NOx interacts with the char particles for a longer period, increasing NOx reduction. Fig. 20, depicts the pressure and temperature effect on char-N oxidation while maintaining an oxygen concentration in the flue gases of up to 5% and N_2 as the balance gas. At atmospheric pressure, the oxidation of char-N to NOx increases dramatically with raising the temperature. However, as pressure rises, the conversion of char-N to NOx decreases, and the impact of temperature weakens. The mechanism of NO_x reduction on the char surface in pressurized oxy-combustion conditions is discussed by Liang et al. [72]. They revealed that in oxy-combustion conditions, with an increase in CO_2 partial pressure at high pressure and temperatures above 900 °C, CO_2 gassification occurs in the presence of char, leading to the formation of CO through the reactions below,

$$CO_2 + C \rightarrow 2CO \qquad (R34)$$

$$2CO_2 \rightarrow 2CO + O_2 \qquad (R35)$$

the generated CO promotes the reduction of NO via R36,

$$2NO + 2CO \rightarrow N_2 + 2CO_2 \qquad (R36)$$

Additionally, the prolonged residence time of NO_x inside the char leads to the heterogeneous reduction of NO to N_2 through R37.

$$2NO + 2C \rightarrow N_2 + 2CO \qquad (R37)$$

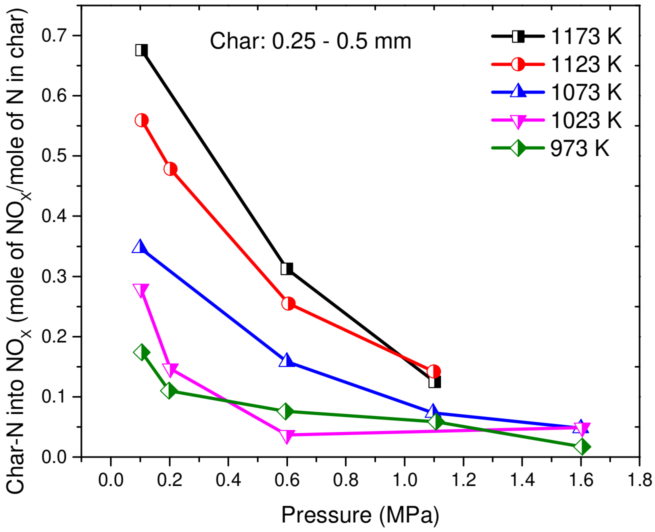

Fig. 20. Impact of pressure and temperature on NOx evolution in char combustion (5% O_2, N_2 as a balance gas) [84].

6. Reduction of NO_x in pressurized oxy-combustion.

Increasingly with time, the requirement to reduce NO_x emission from coal combustion has become more stringent. Different conventional methods are used for the reduction of NOx. For example, staged combustion technologies such as air staging and fuel staging (reburning), flameless combustion, internal recirculation, selective non-catalytic reduction (SNCR), and selective catalytic reduction (SCR). However, all of these NO abatement technologies are used at ambient pressure, and no research has been performed using any of the above technologies at elevated pressure to the best of our knowledge. We explore SNCR and reburning at high pressure and their effectiveness in NOx control based on the numerical simulation.

6.1. Pressurized SNCR (Thermal De-NOx)

Selective non-catalytic reduction is one of the most important and practical methods for lowering NOx in flue gases (SNCR) [139]. Conceptually, in the SNCR method, ammonia, urea [140-143], and cyanuric acid [144-147] are added as reducing reagents into the flue gas stream carrying NO_x [148]. These reagents effectively reduce the NO_x to N_2 by homogeneous gas-phase reaction at a specific temperature range (1100-1250 K) [149, 150]. The SNCR process has multiple advantages over catalytic processes. It is easily applicable without the need for a separate process unit, which reduces the capital cost. Further, it does not require an expensive catalyst, resulting SNCR highly economical compared to the other methods. Furthermore, the SNCR is not typically polluted with fly ash and can be used in combination with other NOx pollution control methods, such as fuel staging, air staging, internal recirculation, and so on [148]. In this work, we limit our discussion to the SNCR process with ammonia, also known as the thermal de-NOx process at high pressure since the reaction mechanism is only available for ammonia as a reducing agent. Several researchers studied the SNCR method at atmospheric pressure with detailed chemistry [42, 124, 137, 151-154]. The main limitation of this process at atmospheric pressure is that it can reduce NO_x only in a narrow temperature window, i.e., 1100-1250 K. At temperatures lower than 1100 K, the rate of NO_x reduction reactions is insignificant while at temperatures higher than 1400 K, NO_x formation rather than reduction is dominant.

However, the impact of high pressure on the SNCR mechanism has not been thoroughly studied. Therefore, to predict and analyze the SNCR process's behaviour at high pressure, we employ a widely developed gas-phase mechanism based on the GRI Mech 3.0 by incorporating the subset of nitrogen chemistry from Glarborg et al. [155] and Mueller et al. [156]. The mechanism included 72 species and 428 elementary reactions. The mechanism can be found in the supplementary materials presented in our previous work [157]. Before using the mechanism for pressurized SNCR, it was first evaluated with the experimental finding from the literature referenced in Table 1 and 2. Under both ambient and elevated pressure, the kinetic model offers a satisfactory prediction of NOx reduction and a relatively good agreement with experimental findings, as shown in Fig. 21 and Fig. 22, respectively. Tables 1 and 2, demonstrate the experimental conditions for Figs. 21 and 22, respectively.

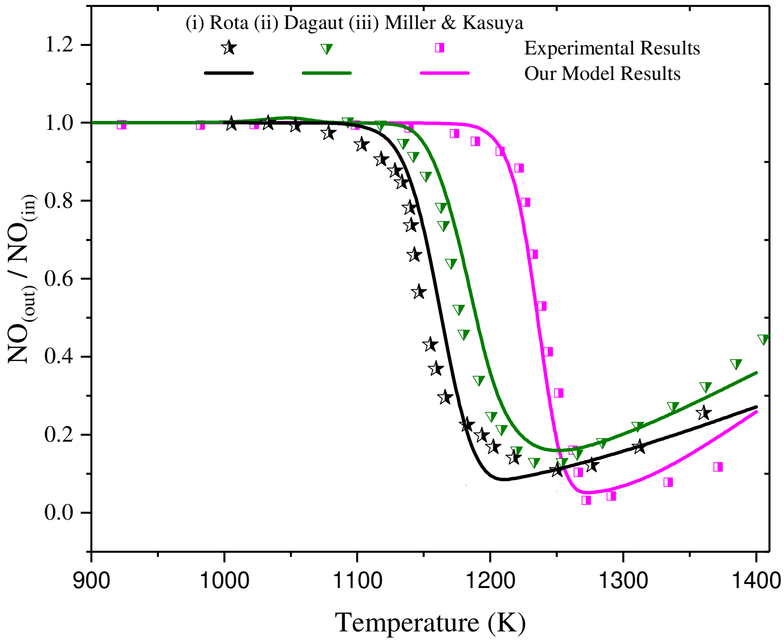

Fig. 21. Evaluation of the experimental and simulation results at atmospheric pressure; experimental conditions are given in Table 1 [150].

Table 1. Boundary conditions of the experimental works used for mechanism evaluation.

Experimental works	boundary conditions at the inlet					
	$\tau_{(s)}$	O_2 (%)	NO (ppm)	H_2O(%)	NH_3 (ppm)	Facility
R.Rota et al. [158]	0.1	0.8	400	0 or 3	960	JSR
Dagaut et al. [159]	0.1	1.25	500	0	1000	JSR
Miller and Kasauya [139, 151]	0.1	0.5	500	5	1000	PFR

$\tau_{(s)}$ = residence time

Table 2. Boundary conditions of the experimental works used for mechanism evaluation

Cond (#)	τ (s)	T (K)	P (atm)	Inlet species	Ref
1	2164/T	1023-1423	1.05	O_2=4.7%, SO_2=510ppm, SO_3=583ppm	[160]
2	2320/T	1023-1423	1.05	SO_2=238 ppm, SO_3=342 ppm, O_2 =4.7%	[160]
3	1	700-1200	10	O_2=0.333%, H_2=1%, NO=220 ppm,	[161]
4	1	700-1200	10	H_2=1%, O_2=1%, NO_2=65 ppm	[161]
5	0-1.5	950	1.2	SO_2=500 ppm, H_2O=0.49%, NO=97 ppm, CO=0.51 %, O_2=0.75%	[162]
6	0-1.5	950	3	SO_2=500 ppm, H_2O=0.49%, NO=97 ppm, CO=0.51 %, O_2=0.75%	[162]
7	0-1.5	950	6.5	SO_2=500 ppm, H_2O=0.49%, NO=97 ppm, CO=0.51 %, O_2=0.75%	[162]
8	0-1.5	950	10	SO_2=500 ppm, H_2O=0.49%, NO=97 ppm, CO=0.51 %, O_2=0.75%	[162]
9	0-1.5	950	10	SO_2=577 ppm, NO_2=204 ppm	[162]

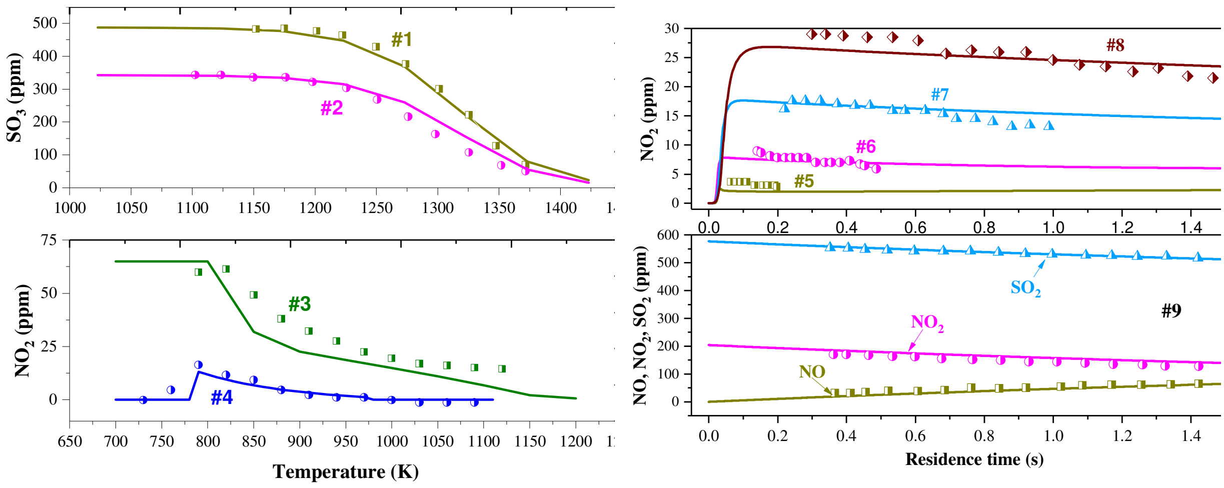

(a) (b)

Fig. 22. Model evaluation with the literature data at elevated pressure. Operating condition are given in Table 2, [163].

Fig. 23, illustrates the pressure effect on the SNCR process at various temperatures. The NO reduction curves at various pressures indicated that NO reduction efficiency improves marginally by about 2 to 3% with elevating the pressure from 1 to 15 atm [157, 164]. However, the optimal temperature window for maximum NO reduction is expanded by 100 K for 5 atm and 150 K for 10 atm, respectively. Following that, the temperature window increases insignificantly above 10 atm, i.e., only a 10 K increase from 10 atm to 15 atm. The benefit of the temperature window expansion in addition to the fact that NOx control can be accomplished over a large operating range of the boiler is that it provides operational versatility in ammonia injection position in the boiler. Expansion of the temperature window at high pressure can be a result of two probable effects, 1) the enhancement of OH radical concentration at high pressure, facilitating the conversion of NH_3 to NH_2 via $NH_3 + OH \rightarrow NH_2 + H_2O$, which further reacts with NO and convert it into N_2 via $NH_2 + NO \rightarrow N_2 + H_2O$ and 2) high pressure suppresses the reaction kinetics of major NO_x formation reactions such as $H + NO + M \rightleftarrows HNO + M$ and $HNO + OH \rightleftarrows NO + H_2O$, at high temperature i.e., at 1400 K where NH_3 oxidation normally starts at 1 atm. The expansion of the temperature window for the SNCR process at higher pressures is indirectly corroborated by the findings from Kasuya et al. [139]. They found that an increase in the partial pressure of the reactants contributes to an increase in the temperature range for NO_x reduction, similar to high-pressure reactions.

The main reaction pathway for NO reduction is shown in Fig. 24. The homogeneous reduction of NO starts with the formation of NH_2 radicals by reactions of ammonia with OH, O, or H atoms;

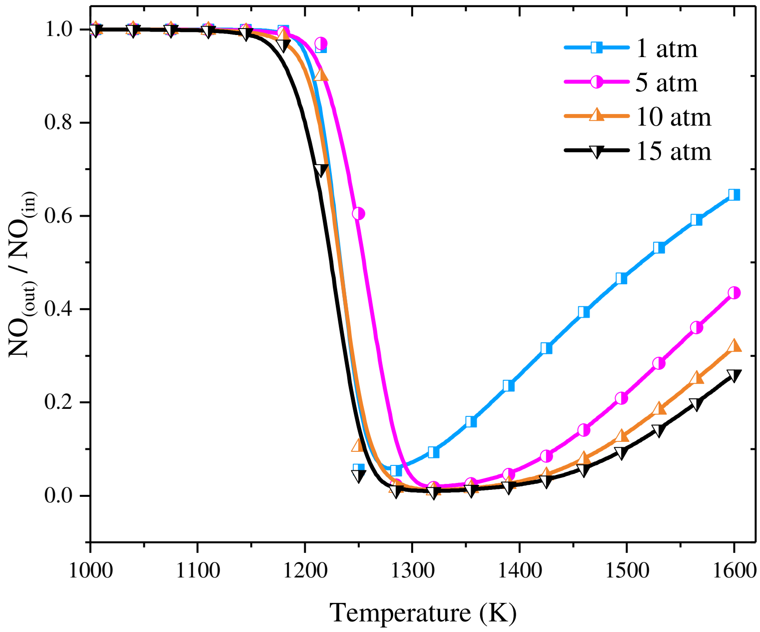

Fig. 23. Pressures effect on NO_x reduction vs temperature: (NO_i=500ppm, NH_3=1000 ppm, O_2=0.5%, H_2O=5%, residence time=0.1 sec, and Ar as a balance gas) [151].

$$NH_3 + OH \rightarrow NH_2 + H_2O \qquad (R38)$$

$$NH_3 + O \rightarrow NH_2 + OH \qquad (R39)$$

$$NH_3 + H \rightarrow NH_2 + H_2 \qquad (R40)$$

The primary elementary reaction of the NO to N_2 conversion is:

$$NH_2 + NO \rightleftarrows OH + NNH \qquad (R41)$$

$$NH_2 + NO \rightarrow N_2 + H_2O \qquad (R42)$$

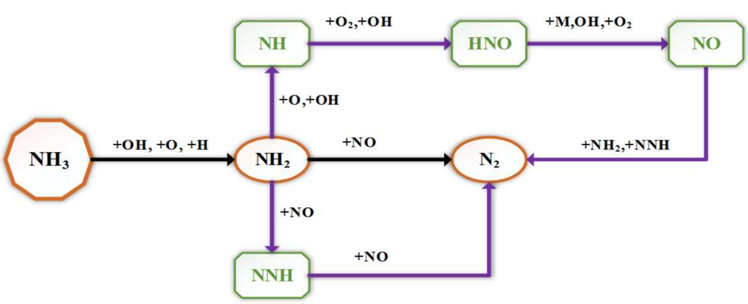

Fig. 24. Reaction pathways of NO reduction in pressurized SNCR process.

6.2 Pressurized Reburning

Reburning is one of the matured technologies used to reduce NO_x as an alternative to the SCR and SNCR processes [165, 166]. In the reburning process, the NO_x is controlled by fuel staging [167, 168]. In the first stage, a large portion of the fuel, approximately 80-90 percent, is combusted in burners with 10 percent excess air in the combustion zone [117]. A significant amount of NO_x is produced in the prime combustion zone. Following the first stage of combustion, 15-25% of the reburning fuel is provided in the secondary zone, also called the reburning zone, to create the fuel-rich condition. Experimental analysis suggests that 50-70% NO_x can be reduced by keeping the air to fuel ratio, residence time, and temperatures in a specified range [169]. Finally, over-fire air (OFA) is added in the third stage to combust the remaining fuel. The reburning fuel produces a fuel-rich atmosphere with controlled hydrocarbon radical concentrations such as CH_3, CH_2, CH, C, HCCO, and so on. These hydrocarbon radicals (CH_i) have the ability to reduce NOx by transforming it into a number of intermediate species with C-N bonds. These intermediate species are further reduced to the NH radicals (NH_2, NH, N) in the presence of CH_i radicles pool and then react with NO to form molecular nitrogen. Thus, NO can be reduced by reactions with two types of species: CH_i and NH_i radicals. Coal, gas, or other fuels can be employed as a reburn fuel [170].

The reburning mechanism has been studied widely at atmospheric pressure both experimentally and numerically. The experimental work published provides data for flow reactors [171-177] and jet-stirred reactors [167, 178-180]. Despite the complex reburning chemistry, the published studies about the modelling of fuel-NO reburning have generally achieved acceptable results, at least for smaller hydrocarbons [42, 44, 167, 171, 172, 174, 179-184]. However, no work has been done to understand the impact of high pressure on reburning processes. Since POC is an emerging technology and has a high efficiency compared to atmospheric combustion, it is important to analyze the reburning process at high pressure to understand its applicability for NO_x control in this technology. We use Chemkin to simulate different reburning gaseous fuels, such as CH_4, CH_4+C_2H_6, C_2H_4, and C_2H_2, because these fuels are lightweight and easily decompose at high temperatures and are commonly used for reburning processes.

Before beginning the study on reburning for NOx control at high pressure, the best mechanism should be selected by comparing multiple mechanism results with experimental data from the literature [185]. Five mechanisms were chosen for this reason, the specifics of which can be found in our previous work [186]. All of these mechanisms are validated under fuel-rich conditions by comparing it with the experimental work [185]. Table 3, summarizes the total reactions, species, and references of the selected mechanisms. As shown in Fig. 25, PG 2018 calculates very acceptable and similar results to the experiment. As a result, PG 2018 has been chosen for additional validation under high pressure. Table 4, summarizes various experimental conditions at high pressure selected from the literature to validate the PG 2018 in pressurized conditions and different equivalence ratios. Fig. 26, shows that the PG 2018 simulated findings are very close and in good agreement with experimental results at high pressure, for all equivalence ratios. As a result, it was eventually agreed to use PG 2018 to study the reburning process at ambient and elevated pressure conditions.

Table 3. Five mechanisms used for validation with the experimental results

Mechanism	Species	Reactions	Ref
GRI 3.0	53	325	[187]
P. Dagaut	145	1006	[179]
GRI 2.11	49	279	[188]
PG 2018	151	1397	[117]
KONNOV 0.6	129	1231	[189]

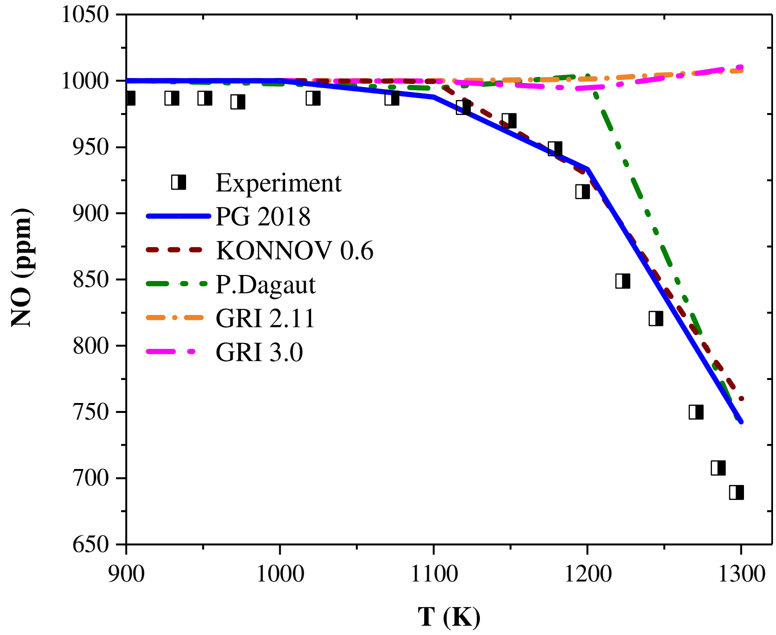

Fig. 25. Validation of different mechanisms with experimental finding at atmospheric pressure, using JSR facility [186]. Operating conditions are given in Table 4.

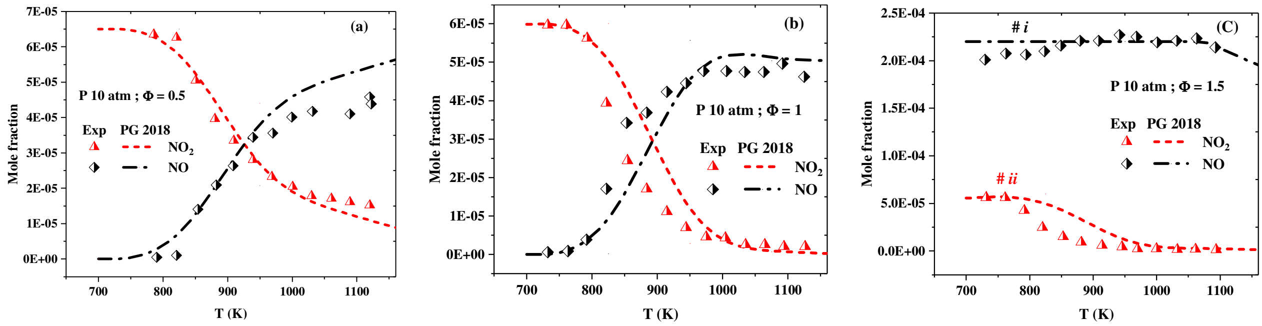

Fig. 26. Evaluation of "PG 2018" simulation results with the experimental results at elevated pressure and different equivalence ratio; (a) fuel-lean (b) stoichiometric ratio (c) fuel-rich [186]. Operating conditions are given in Table 4.

Table 4. Experimental inlet conditions from literature used for mechanism validation

Fig #	$(\Phi)^*$	τ (s)*	P (atm)	Inlet compositions	Ref
25	1.43	3.59	1	CO_2=30%, CH_4= 1000 ppm, NO=1000 ppm, N_2 balance gas	[185]
26 (a)	0.5	1	10	H_2=1%, O_2=1%, NO_2=65 ppm	[161]
26 (b)	1	1	10	H_2=1%, O_2=1%, NO_2=60 ppm,	[161]
26 (c) # *i*	1.5	1	10	H_2=1%, O_2=0.333%, NO=220 ppm	[161]
26 (c) # *ii*	1.5	1	10	H_2=1%, O_2=1%, NO_2=60 ppm	[161]

* $\tau_{(s)}$ = residence time, Φ = equivalance ratio

The effect of pressure ranging from 1 to 15 atm on the reburning process is investigated using a chemkin simulation based on the Glaborg mechanism. The results calculated through simulation are shown in Fig 27. The results suggest that from the baseline case of 1atm, the concentration of NO_x decreases with an increase in pressure. The effect of pressure up to 10 atm is significantly high compared to the effect above 10 atm. The decrease in NO with increased pressure during reburing is a possible result of high pressure favouring the formation of high concentrations of CH_i and NH_i radicals, which then react readily with

NO. From ROP analysis, the most important reactions that are involved in the formation of reactive radicals, i.e., CH_i and NH_i, from reburning fuels are;

$$CH_4 + OH \rightleftarrows CH_3 + H_2O \qquad (R43)$$

$$CH_4 + H \rightleftarrows CH_3 + H_2 \qquad (R44)$$

$$CH_4 + O \rightleftarrows CH_3 + OH \qquad (R45)$$

$$CH_4 + CN \rightleftarrows CH_3 + HCN \qquad (R46)$$

For NHi

$$HNCO + H \rightleftarrows NH_2 + CO \qquad (R47)$$

$$CH_3 + H_2NO \rightleftarrows CH_3O + NH_2 \qquad (R48)$$

When ethane is used as a reburning fuel, the reactive radicals form by the following reactions;

$$C_2H_6 + OH \rightleftarrows C_2H_5 + H_2O \qquad (R49)$$

$$C_2H_6 + H \rightleftarrows C_2H_5 + H_2 \qquad (R50)$$

$$C_2H_6 + CN \rightleftarrows C_2H_5 + HCN \qquad (R51)$$

$$C_2H_6 + NCO \rightleftarrows C_2H_5 + HNCO \qquad (R52)$$

The reactive radicals from reburning fuel react and reduce the NO in flue gases with the following reactions;

$$NH_2 + NO \rightleftarrows N_2 + H_2O \qquad (R53)$$

$$NH_2 + NO \rightleftarrows NNH + OH \qquad (R54)$$

$$NO + H(+M) \rightleftarrows HNO(+M) \qquad (R55)$$

$$CH_3 + NO \rightleftarrows HCN + H_2O \qquad (R56)$$

$$HCCO + NO \rightleftarrows HCNO + CO \qquad (R57)$$

$$HCCO + NO \rightleftarrows HCN + CO_2 \qquad (R58)$$

$$CH_3 + NO \rightleftarrows H_2CN + OH \qquad (R59)$$

$$NCO + NO \rightleftarrows N_2 + CO_2 \qquad (R60)$$

From reaction path analysis, the main reaction pathway is shown in Fig. 28. The arrows' thickness denotes the importance of the reactions.

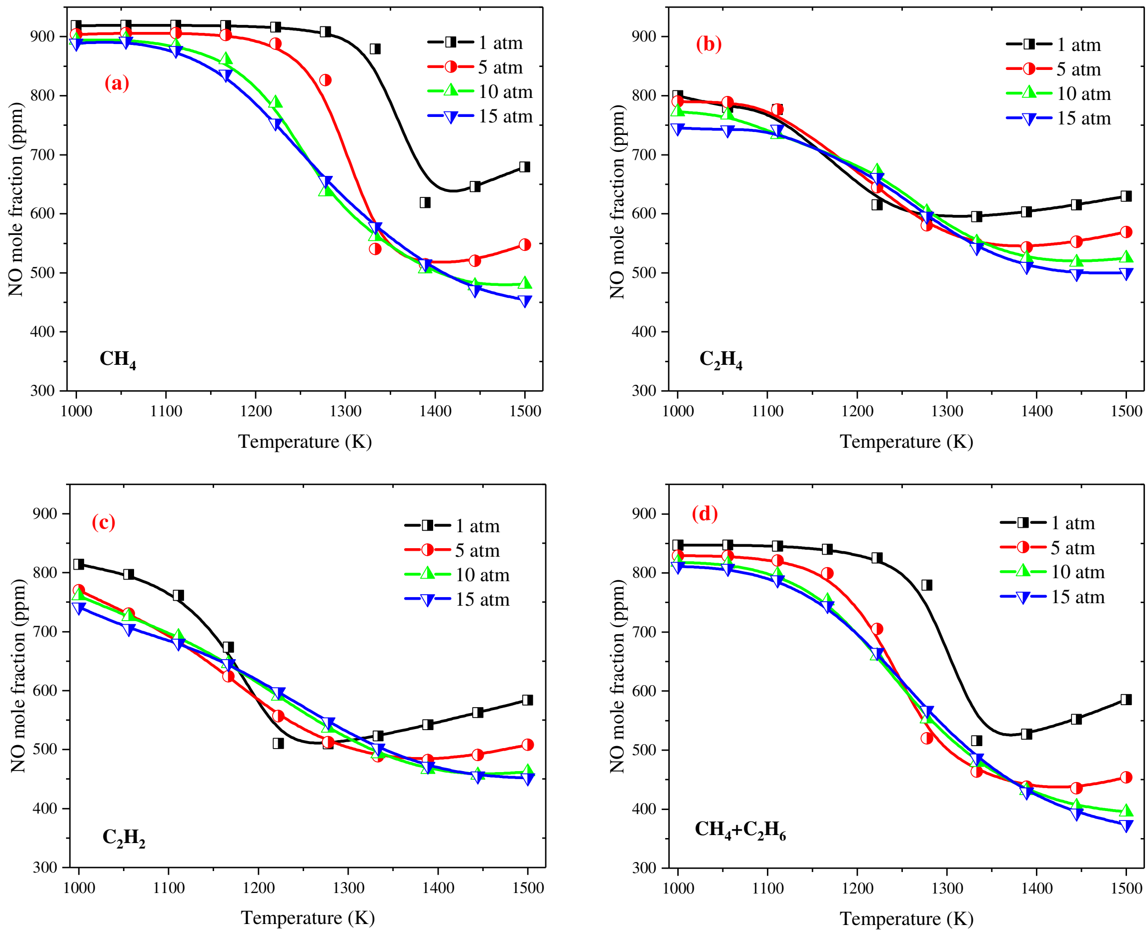

Fig. 27. Pressure effect on NO reduction by different hydrocarbons during the reburning process, using a simulated PFR. Inlet stream condition: (a) NO = 920 ppm, O_2 = 4830 ppm, CH_4 = 2800 ppm, (t = 0.15 sec); (b) NO = 790 ppm, O_2 = 2015 ppm, C_2H_4 (ethylene) = 1020 ppm, (t = 143 sec); (c) NO = 835 ppm, O_2 = 1700 ppm, C_2H_2 (acetylene) = 890 ppm, (t = 14 sec); (d) NO = 850 ppm, O_2 = 4885 ppm, CH_4 = 2770 ppm, C_2H_6 = 260 ppm, (t = 0.14 sec).

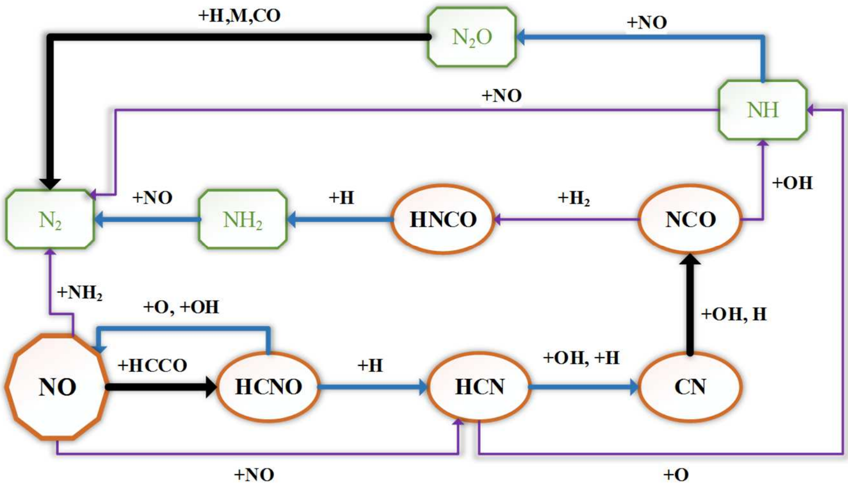

Fig. 28. Reaction pathway of NO reduction by reburning with methane and ethane.

6.3. Effect of pressure on the conversion of NO to NO_2

The separation of acid gas contaminants (NOx and SOx) and recovery of latent heat of vapors are primarily carried out in a single integrated direct contact (DCC) wash column in the developing technique (SPOC). DCC removes NOx and SOx at a low cost because it eliminates the need for two separate systems, such as SCR and flue gas desulphurization [29]. DCC readily absorbs NO from flue gas in the form of NO_2 since NO_2 is easily soluble in water compared to NO [82, 190]. Furthermore, it can easily oxidize SO_2 to SO_3 or H_2SO_3 to H_2SO_4 through SOx/NOx reactions in gas or liquid [191].

NO_2 is typically produced at high pressure and lower temperature region (in post flame temperature) [192]. However, NO_2 formation in the combustion phase has received little attention, owing to the fact that NO_2 is highly susceptible to high temperatures, and only a small amount is produced in the post-flame area at atmospheric pressure [193]. There have only been a few studies on the emission of NO_2 in the post-flame condition region at high pressure. Mueller et al. [194], analyzed the overall impact of NO on fuel oxidation and high-pressure conversion of NO to NO_2, concluded that NO to NO_2 oxidation is highly dependent on pressure and stoichiometry (oxygen concentration). Hori et al. [195], investigated the hydrocarbons influence on the conversion of NO to NO_2 at the atmospheric pressure and temperature ranging from 600-1100 K. They reported that hydrocarbon has the ability to enhance the conversion of NO to NO_2, mainly through the reaction R61 (HO_2+NO=NO_2+OH). Furthermore, they discovered that the hydrocarbon effect on NO_2 conversion is highly dependent on fuel type and reaction temperature. Mueller et al. [162], went on to investigate the relationship between SO_2 and NO in the O_2/NO/SO_2/H_2O/CO system at pressures and temperatures ranging from 0.5 to 10.0 bar and 950 to 1040 K, respectively. They inferred that at elevated pressures, where the NO conversion to NO_2 rises, the reaction R62 (SO_2+NO_2 = SO_3+NO) is also significant and cannot be underestimated.

Several studies have reported that NO interacts with HO_2 radical via reaction R1 to produce NO_2 [196, 197]. Hence, the conversion of NO to NO_2 increases with the increase in HO_2 concentration. A major route for HO_2 formation is R63 ($H + O_2 + M \rightleftarrows HO_2 + M$) [42, 197, 198], which, being a three-body reaction, is highly sensitive to pressure. Further, this reaction is also influenced at low temperatures [199]. In effect, NO to NO_2 is prone to high pressure and relatively low temperatures. Hunderup et al. [200], studied the impact of pressure, temperature and methane injection on NO to NO_2 conversion. The NO_2/NO profiles as a function of pressure are shown in Fig. 29 (a), indicating that NO to NO_2 conversion increased with pressure, with maximum formation at 8.54 atm. They also reported that methane enhanced the NO oxidation by increasing the concentration of HO_2 radical. Similar timothy ting et al. [82], studied the NO oxidation to NO_2 at laboratory scale experiment and then solved it in liquid water at high pressure and oxy-fuel condition, and the result is shown in Fig. 29 (b). This conclusion is supported by our research group numerical analysis at high pressure [199], as shown in Fig. 30 (b). We observe that at both 900 ºC and 1000 ºC, NO_2 formation increases with the increase in pressure from 1 bar to 15 bars. Moreover, the NO_2 production is much higher in POC conditions than in atmospheric-combustion. It is concluded from ROP analysis that NO_2 is mainly produced by reactions R61 (HO_2+NO=NO_2+OH), R64 (NO+O+M=NO_2+M), R65 (NO+O_2=NO_2+O), and R66 (NO_2+HO_2=HONO+O_2). However, the impacts of these reactions are significantly pressure and temperature dependent. At ambient pressure and high temperature, reaction R64 occurs in the reverse direction and reacts with NO_2, formed via reaction R61 from the oxidation of HO_2, where the effect of reaction R67 (O_2+H_2O=OH+HO_2) is significant. However, at elevated pressure and lower temperature, reaction R64 reacts in the forward direction and facilitates the NO_2 production, comparatively higher than reaction R61.

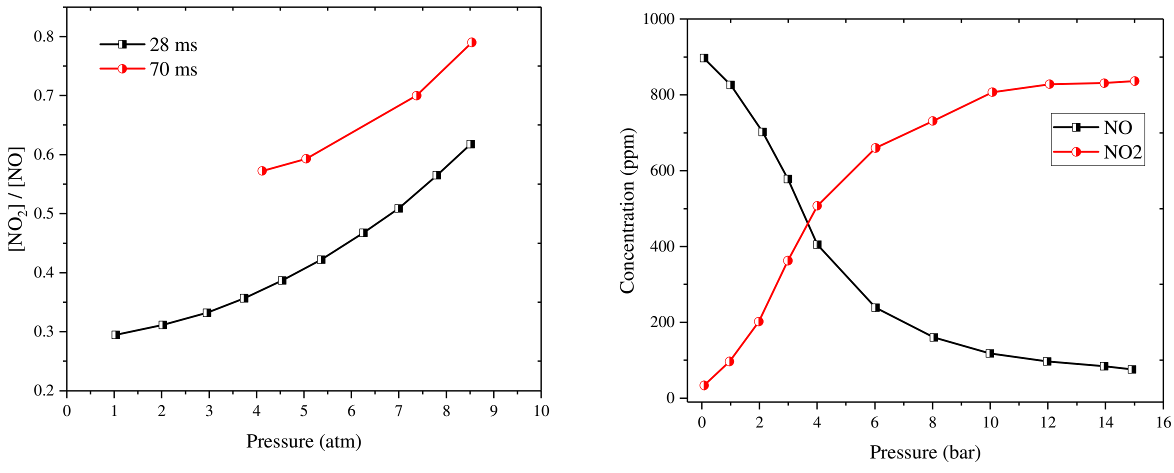

(a) (b)

Fig. 29. Effect of pressure on NO oxidation to NO_2, experimental work by (a) [200] and (b) [82] respectively.

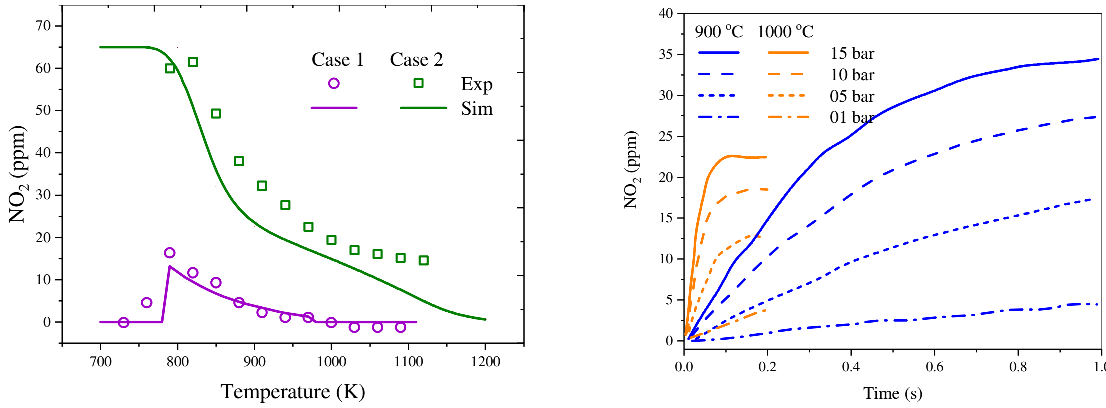

(a) (b)

Fig. 30. (a) Validation of our mechanism used for numerical calculations, initial conditions: 1 s, 10 atm, 1% H_2, case 1: 220 ppm NO, 0.333% O_2; case 2: 65 ppm NO_2, 1% O_2 [201] (b) Effect of pressure on NO_2 formation at two temperature (900 °C,1000 °C) and pressure (1bar,10 bar) respectively.

6.4. Direct contact column (DCC)

Using DCC technology, pressurized combustion has the ability to remove NOx and SOx in a more cost-effective manner than conventional removal methods, such as selective catalytic reduction (SCR) for NOx and flue-gas desulfurization (FGD) for SOx [202]. Researchers have found that an elevated pressure (usually above 15 bar) can activate certain gas-phase reactions that enable simultaneous NO_x and SO_x removal in simple water wash columns.

This finding was first proposed to remove NO_x and SO_x from atmospheric oxy-combustion systems, where the flue gas was cooled and compressed and then fed into reactive-absorption columns [203-206]. Air products proposed a two-stage system, where cold flue was compressed to 15 bar and sent to a wet scrubber to remove most of the SO_2 and up to 80% of NO_x, then the partially cleaned flue gas was further compressed to 30 bar, and another wet scrubber was used to remove the remaining NO_x. Air-Liquide [203, 204] and Praxair [206] also proposed similar processes for pollutant removal. Even though this concept is promising, the presence of moisture in the flue gas can results to an acid condensation during compression, which brings in challenges for the compressors. However, using this approach in pressurized oxy-combustion (POC) can avoid this problem as there is no need for flue gas compression. Washington University in St. Louis is working on a DCC that can extract NOx and SOx directly from the warm flue gas of pressurized combustion while also recovering the heat energy from the flue gas moisture by condensing it into a liquid which leads to improving plant efficiency [207, 208]. A pilot-scale system at a flue gas temperature of 200 ^{o}C has been demonstrated, and the results are promising. A simplified process diagram of a POC plant employing DCC as the SO_x and NO_x removal unit is shown in Fig. 31.

The SO_x and NO_x reactive-absorption process under pressure takes place in three phases: 1) the gas-phase reaction between NO and excess O_2 to produce NO_2; 2) the interphase absorption of NO_x and SO_x in water, and 3) reaction of sulfur- and nitrogen-containing species in the liquid phase.

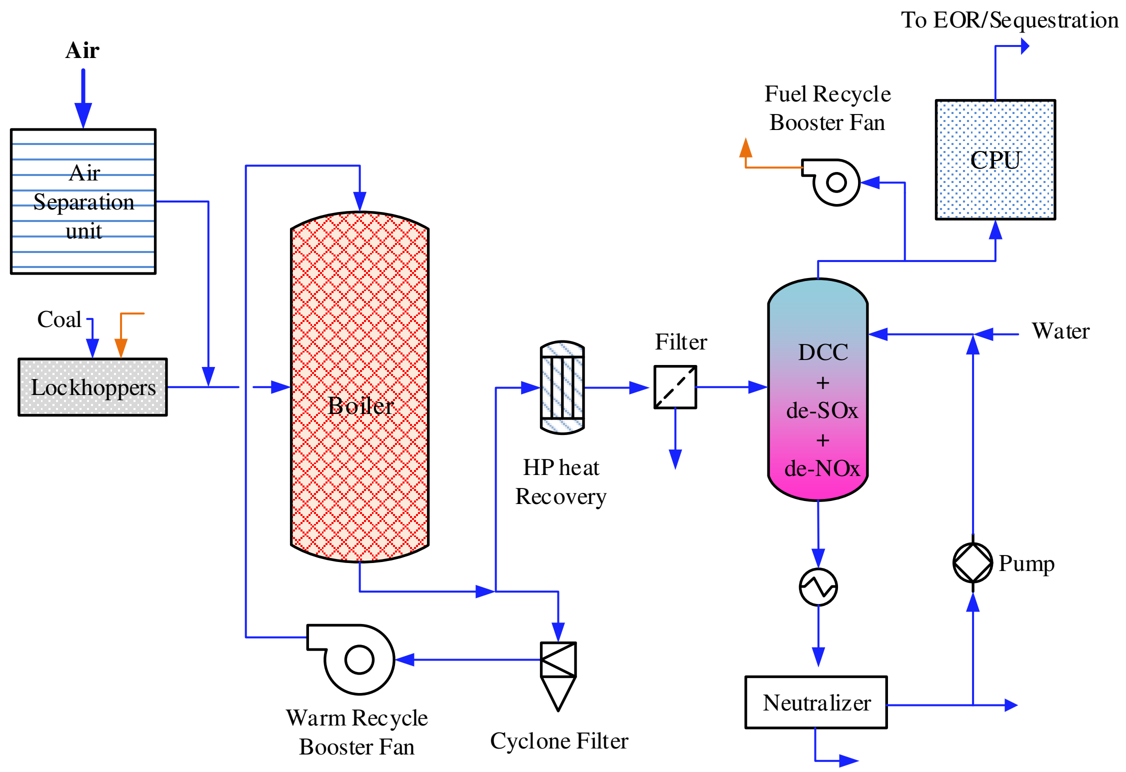

Fig. 31. A simplified process diagram of a POC plant employing DCC as the SOx and NOx removal unit.

Norman et al. [191], presented the detailed chemical reaction mechanism inside a DCC column in both gas and liquid phase with 33 reactions including several intermediate reactions; however, several of the reactions considered in the mechanism existed in insignificant amount. Based on the equilibrium and sensitivity analysis in pressurized flue gas systems, Ajdari et al. [209], reduced Normann et al. mechanism significantly, claiming that the NO oxidation to NO_2 controls the removal of NO, with SO_x removal controlled through the liquid phase reaction between absorbed SO_2 and NO_2. Verma et al. [207], further reduced the mechanism to a 5 reaction system based on experimental results and modelling and agreed with Ajdari et al. on the limiting step. Axelbaum et al. [208], also performed pilot scale studies in a direct contact column for NO and SO_2 removal at 15 bar and multiple temperatures. They supported the results with the model based on the previously developed mechanism [207]. They reported that NO oxidation indeed limits the removal of NO and SO_2. However, they saw small disagreements at higher gas temperatures.

Since the interphase absorption equilibrium for both SO_2 and NO_2 is well established [210], a brief review of the reactions controlling the removal of SO_x and NO_x in gas and liquid phases is discussed below.

6.4.1. Gas-phase reactions in DCC

The kinetics of NO oxidation at temperatures specific to DCC have been widely investigated and are well known. Tsukahara et al. conducted a detailed review of the NO oxidation kinetics in the dry gas phase, where they illustrated that the reaction is a third-order homogenous reaction with an Arrhenius equation, k ($L^2.mol^{-2}.s^{-1}$) $= 1.2 * 10^3 \exp\left(\frac{530}{T}\right)$, with the best fit between the temperatures of 273 K and 600 K [211]. As evident from the equation, several studies reported in the review found out that the temperature dependency of the rate constant is marginally inverse. In other words, the rate decreases with increasing temperature.

$2NO + O_2 \rightarrow 2NO_2$

Murciano et al. [212], studied the chemical reactions in a sour gas compression process in both dry and wet conditions. While carrying out experiments in a room-temperature CSTR reactor under varying pressures (5-15 bar) and varying residence times (0.5-750 s), they found that NO is easily oxidized to NO_2 in the presence of oxygen. Ting et al. [82], conducted similar room-temperature CSTR experiments for dry gas-phase oxidation of NO to NO_2 with a pressure ranging from 1 to 31 bar and a corresponding change in residence time from 12.3 to 375.2 s. With an inlet concentration of 900 ppm of NO and 4% O_2, the results portrayed that the increase in pressure (and a simultaneous increase in residence time) enhances the conversion of NO to NO_2. Ting et al. also reported that NO oxidation is kinetically limited under these conditions as the conversion increased with increasing residence time. Under these conditions, they reported a kinetic rate constant k ($L^2.mol^{-2}.s^{-1}$) $= 2.4 * 10^3 \exp\left(\frac{530}{T}\right)$, which is similar to the one reported by Tsukahara et al. Cheng et al. [213], performed a regression analysis of the existing kinetics and experimental results to ascertain the rate constant applicable for high pressure NO oxidation pressure (1 – 3 MPa), they found that there is small reversibility to the reaction and reported that the rate of NO_2 formation as:

$$\frac{d[NO]}{dt} = 3.4\,[NO_2]^2 - 2.6\,[NO]^2[O_2]$$

Other oxides of nitrogen, including N_2O_4, N_2O_3, and N_2O, were neither identified by lab-scale experiments[214, 215] nor measured[82] [13]. Murciano et al. and Ting et al. considered the oxidation of NO to NO_2 as the most important (or the only) NO_x reaction in the gas phase.

6.4.2. Liquid phase reactions

SO_2 is absorbed in water to form HSO_3^-, and NO is oxidized to NO_2 and then absorbed in water to form HNO_2 and HNO_3. Their reaction rates determine the removal of NO_2 and SO_2 from the gas phase. Chang et al. [216], proposed the most comprehensive liquid phase reaction mechanism between HSO_3^- and HNO_2, presented in Fig. 32. The reaction between HNO_2 and HSO_3^- produced the intermediate nitrosylsulfuric acid (NSS), whose subsequent reactions depend on the pH of the solution and the relative concentrations of the reactants in the solution. The possible three pathways for NSS are 1) reaction with HSO_3^- to produce hydroxylamine di-sulfonate (HADS); 2) Direct hydrolysis of NSS to form sulfuric acid and nitrous oxide (N_2O); 3) reaction of NSS with nitrous acid to form sulfuric acid and nitric oxide. Oblath et al. [217, 218], studied the impact of pH on the three reactions and reported that the hydrolysis reaction of NSS was observed below the pH of 3.2, resulting in the formation of N_2O, and HADS was the sole product above the pH of 4. The study was limited to room temperature and did not propose the kinetics below the pH of 4.

Susianto et al. [219], studied the interaction between HNO_2 and HSO_3^- ions in a similar setup and reduced the mechanism to two major reactions shown in Fig. 33. They reported that below pH of 1, only sulfuric acid and N_2O are produced (pathway 3), and above pH of 4, only HADS is produced (pathway 2). They concluded that, between pH of 1 and 4, both reactions take place with the selectivity depending on the pH. The study was limited to room temperature, and kinetics below pH of 4 was not proposed.

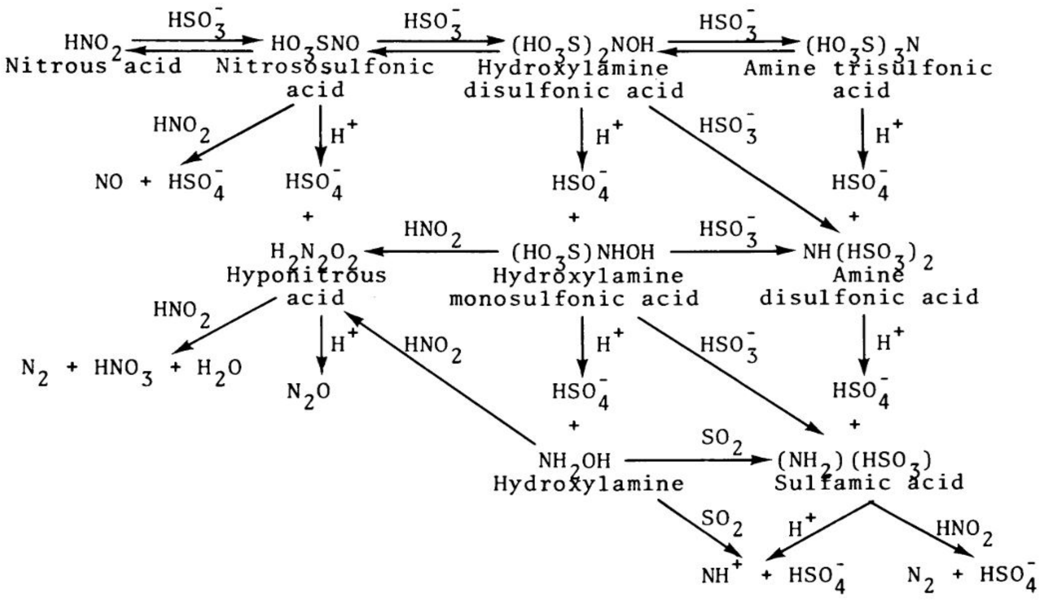

Fig 32. Reaction mechanism proposed by Chang et al. [216]

$$HNO_2 + HSO_3^- \xrightarrow{1} NSS \xrightarrow{2} HADS \longrightarrow Y$$

$$NSS \xrightarrow{3} N_2O$$

Fig. 33. Reduced liquid phase mechanism illustrated by Susianto et al. [219]. Y represents the product of its acidic hydrolysis whose composition is ill-defined.

Axelbaum et al. [208], analyzed the kinetics of the reaction between HNO_2 and HSO_3^- relevant to DCC conditions at a pH between 2 and 4 and a temperature range of 20 – 90 °C. They reported that the first step of the reaction leading to NSS formation is the slow step in the liquid phase and proposed the reaction rate constant of the reaction for studied experimental conditions. They also found that at higher temperatures, HADS decomposes slowly to produce H_2SO_4 and an unidentifiable nitrogen specie.

6.5. Heterogeneous reduction of NOx on char surfaces in pressurized oxy-combustion.

The heterogeneous reduction of NO_x on char surfaces at high pressure was studied by Croiset et al. [58]. They predicted the effect of pressure on the rate of NO reduction reaction, as shown in Fig. 34.

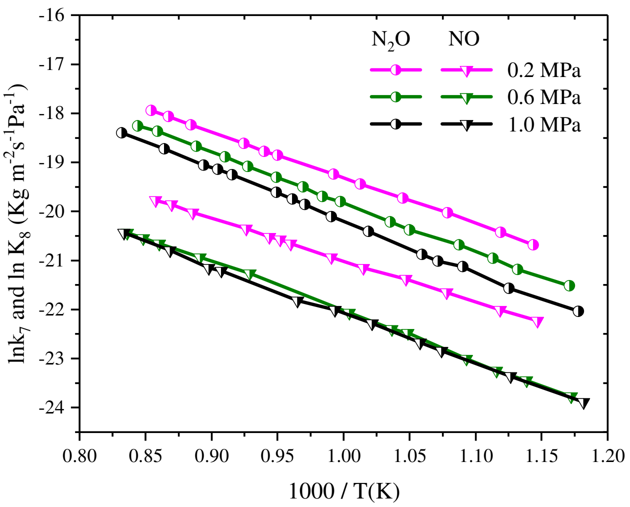

Fig. 34. Arrhenius plots giving the rate constants for NO (k_7) and N_2O (k_8) reacting with Westerholt char [58].

They observed that the rate constant of N_2O reduction was larger than the rate constant for NO reduction up to the pressure of 1.0MPa. Thus, N_2O was quickly reduced on interacting with char as compared to NO. The result is supported by the analysis from De Soete et al. and Rodriguez et al. [220, 221]. As evident in Fig. 34, the influence of pressure is strong up to 0.6 MPa, with a small change between 0.6 MPa and 1 MPa. It is essential to understand how the partial pressures of NO and N_2O change with the total pressure because the reduction of NO and N_2O is influenced not only by the rate constant but also by its partial pressures. An increase in the total pressure would boost the partial pressure of NO and facilitate the reduction of NO on char surface, generating either N_2 or N_2O via the subsequent reaction NO + (-C) => 0.5 N_2 + (-CO) and NO + (-CNO) => N_2O + (-CO). According to Croiset et al. [58], there is no impact of the total pressure on the formation of NO, but it affects the reduction of NO on the char. Hence, the overall NO emission decreases when the total pressure is increased [58]. Jiaye et al. [222], investigated the char morphology in high-pressure pyrolysis utilizing CO_2 as an environment, concluding that the CO_2 gassification reaction considerably enhances char porosity and BET surface area. It means that at higher pressures, the heterogeneous NOx reduction with char might be greatly increased. However, further research is required to explore the impact of high pressure on heterogeneous NO reduction on char surfaces.

7. Conclusion

This paper provides a literature review on nitrogen evolution, NOx formation, and reduction in pressurized oxy-coal combustion. The main conclusions are as follows:

- Coal-N is distributed into volatile-N and char-N during the first step of the thermal conversion process. In devolatilization, the coal-N is first released as tar, which is a mixture of complex structured hydrocarbons and aromatic compounds. The tar-N subsequently converts into HCN and other light gases at high temperatures via secondary pyrolysis. The release of coal-N in tar increases with the heating rate and reduces with pressure.

- Pressure reduces the volatiles of fuel at the initial stages of pyrolysis and prevents its diffusion through the particles. As a consequence, tar can react with char to a larger extent compared to atmospheric pressure and can initiate secondary exothermic reactions. The secondary reactions can result either in cracking, which releases light hydrocarbons, or re-polymerization, which increases char.

- Higher pressure promotes the gasification of CO_2 in the presence of char, resulting in the production of more reducing gases like CO, which improves NOx reduction around the char particles. Furthermore, O_2 transport to the char surface is inhibited, and the residence period of NO within the char particle is prolonged, both of which hinder NO production and improve NO reduction.

- The optimum temperature for NH_3 and HCN oxidation shifts towards a lower value at higher pressure. The concentrations of NO and N_2O decrease while the intermediate HNCO and CO_2 increase, respectively, with pressure. There is a strong effect of pressure up to 10 atm and a diminishing effect above it.

- The de-NO_x efficiency of pressurized SNCR increases by 2-3% with an increase in pressure, but the optimum temperature window expands significantly, i.e., from 1250K to 1450K, which provides flexibility for the location of the SNCR injection system.

- In pressurized reburning, the concentration of NO_x decreases with an increase in pressure. Similar to NH_3 and HCN oxidation, there is a stronger effect of pressure up to 10 atm. The decrease in NO concentration with increased pressure is because high pressure favours CH_i and NH_i radical formation, which reacts readily with NO.

- The conversion of NO to NO_2 increases at relatively low temperatures and elevated pressure. This helps NO_x removal since NO_2 is relatively more soluble in water at a higher pressure than NO. Direct contact cooler (DCC) is an emerging technology that can remove NO_x and SO_x directly from the warm flue gas of pressurized combustion and simultaneously recover the latent heat of the moisture in the flue gas so as to improve the plant efficiency.

8. Future perspectives and Recommendations

Based on this review, we recommended further research to reduce and optimize NO_x in POC. In order to develop methods to control and reduce NO_x production during POC, there needs to be a precise understanding of the modes of formation of NO_x at high pressure. There are limited studies on the impact of pressure on nitrogen evolution between volatiles and char during coal pyrolysis at high pressure. Since, the NOx formation mechanisms from volatile-nitrogen and char-nitrogen are different; therefore, this distribution is important. In addition, NO_x is formed mainly from the homogeneous and heterogeneous oxidation of the major NO_x precursors (HCN, NH_3) and char-N repectively. Despite the fact that this work attempts to predict and understand the homogeneous oxidation of NOx precursors, a deeper analysis, both numerically and experimentally, is required to expand our understanding of the oxidation of NOx precursors at high pressure. Similarly, the heterogeneous oxidation of char-N at high pressure requires more research to explore the NO_x evolution in POC. Furthermore, researchers needed to investigate whether the combination of alkali metals, heavy metals, and SO_2 could be effective on NOx formation from homogeneous and heterogeneous oxidation of NOx precursors and char-N, respectively, and subsequent reduction.

This review also highlights the need for further research on NO_x abatement technologies in POC. Homogeneous and heterogeneous reductions of NO_x are the two key methods to control NO_x during combustion processes. A comprehensive understanding of reaction parameters is required to design NO_x reduction technologies. SNCR and reburning are the two matured technologies currently used for NO_x abatement but have not been extensively studied at high pressure. Similarly, as char porosity becomes more prominent at higher pressure, it can provide a large surface area for heterogeneous reduction. Therefore, focuses should also be given to the heterogeneous reduction of NO_x at high pressure. Further, DCC technology at high pressure is highlighted in this study for the removal of NO_x and SO_x simultaneous by contacting the gases and water. There are still many challenges unsolved in this emerging technology at high pressure like the good contact of gases and liquid, improvement in mass transfer between two phases, enhancement in solubility of NO_x in water, etc.

Declaration of competing interest

The authors state that they have no known competing financial interests or personal ties that could have influenced the research presented in this study.

Acknowledgment

The authors gratefully acknowledge the National Natural Science Foundation of China (Nos. 51761125012), and the Natural Science Basic Research Plan in Shaanxi Province of China (2021JC-03) for financial support. We would like to thank Prof Richard L. Axelbaum and Zhiwei Yang from Washington University in St. Louis for their supportive advice and thorough analysis of the manuscript. Profs Wang and Vujanović greatly acknowledge the China-Slovenia bilateral project *Co-firing of alternative fuels in pulverized coal-fired furnaces*.

References

[1] Chang Q, Gao R, Li H, Yu G, Wang F. Effect of CO_2 on the characteristics of soot derived from coal rapid pyrolysis. Combustion and Flame. 2018;197:328-39.
[2] Li C-Z. Some recent advances in the understanding of the pyrolysis and gasification behaviour of Victorian brown coal. Fuel. 2007;86:1664-83.
[3] Dagaut P, Glarborg P, Alzueta MU. The oxidation of hydrogen cyanide and related chemistry. Progress in Energy and Combustion Science. 2008;34:1-46.
[4] Petroleum B. BP Statistical Review of World Energy Report. BP: London, UK. 2019.
[5] Wu X, Chen G. Coal use embodied in globalized world economy: From source to sink through supply chain. Renewable and Sustainable Energy Reviews. 2018;81:978-93.
[6] Deng L, Jin X, Zhang Y, Che D. Release of nitrogen oxides during combustion of model coals. Fuel. 2016;175:217-24.
[7] Govindaraju VGRC, Tang CF. The dynamic links between CO_2 emissions, economic growth and coal consumption in China and India. Applied Energy. 2013;104:310-8.
[8] Scheffknecht G, Al-Makhadmeh L, Schnell U, Maier JR. Oxy-fuel coal combustion—A review of the current state-of-the-art. International Journal of Greenhouse Gas Control. 2011;5.

[9] Chen L, Yong SZ, Ghoniem AF. Oxy-fuel combustion of pulverized coal: Characterization, fundamentals, stabilization and CFD modeling. Progress in Energy & Combustion Science. 2012;38:156-214.
[10] Buhre BJ, Elliott LK, Sheng C, Gupta RP, Wall TF. Oxy-fuel combustion technology for coal-fired power generation. Progress in energy and combustion science. 2005;31:283-307.
[11] Shaddix CR. Coal combustion, gasification, and beyond: Developing new technologies for a changing world. Combustion and flame. 2012;159:3003-6.
[12] Li L, Duan L, Yang Z, Zhao C. Pressurized oxy-fuel combustion characteristics of single coal particle in a visualized fluidized bed combustor. Combustion and Flame. 2020;211:218-28.
[13] Ndibe C, Spörl R, Maier J, Scheffknecht G. Experimental study of NO and NO_2 formation in a PF oxy-fuel firing system. Fuel. 2013;107:749-56.
[14] Zhang J, Rahman ZU, Wang X, Wang Z, Li P, Wang Y, et al. Hot corrosion behaviors of TP347H and HR3C stainless steel with KCl deposit in oxy-biomass combustion. Journal of Environmental Management. 2020;263:110411.
[15] Wang X, Zhang J, Wang Z, Wang Y, Vujanović M, Tan H. Experimental and kinetics study on SO_3 catalytic formation by Fe_2O_3 in oxy-combustion. Journal of environmental management. 2019;236:420-7.
[16] Skeen SA, Kumfer BM, Axelbaum RL. Nitric Oxide Emissions during Coal and Coal/Biomass Combustion under Air-Fired and Oxy-fuel Conditions. Energy & Fuels. 2010;24:4144-52.
[17] Toftegaard MB, Brix J, Jensen PA, Glarborg P, Jensen AD. Oxy-fuel combustion of solid fuels. Progress in energy and combustion science. 2010;36:581-625.
[18] Escudero AI, Espatolero S, Romeo LM, Lara Y, Paufique C, Lesort A-L, et al. Minimization of CO2 capture energy penalty in second generation oxy-fuel power plants. Applied Thermal Engineering. 2016;103:274-81.
[19] Hong J, Field R, Gazzino M, Ghoniem AF. Operating pressure dependence of the pressurized oxy-fuel combustion power cycle. Energy. 2010;35:5391-9.
[20] Hong J, Chaudhry G, Brisson J, Field R, Gazzino M, Ghoniem AF. Analysis of oxy-fuel combustion power cycle utilizing a pressurized coal combustor. Energy. 2009;34:1332-40.
[21] Zebian H, Gazzino M, Mitsos A. Multi-variable optimization of pressurized oxy-coal combustion. 2012.
[22] Gazzino M, Riccio G, Rossi N, Benelli G. Pressurised oxy-coal combustion Rankine-cycle for future zero emission power plants: Technological issues. ASME 2009 3rd International Conference on Energy Sustainability collocated with the Heat Transfer and InterPACK09 Conferences: American Society of Mechanical Engineers Digital Collection; 2009. p. 881-92.
[23] Zebian H, Mitsos A. Pressurized OCC (oxy-coal combustion) process ideally flexible to the thermal load. Energy. 2014;73:416-29.

[24] Malavasi M, Landegger G. Optimization of Pressurized Oxy-Combustion with Flameless Reactor. Unity Power Alliance, LLC, Worcester, MA (United States); 2014.
[25] Zebian H, Rossi N, Gazzino M, Cumbo D, Mitsos A. Optimal design and operation of pressurized oxy-coal combustion with a direct contact separation column. Energy. 2013;49:268-78.
[26] Yang Z, Khatri D, Verma P, Li T, Adeosun A, Kumfer BM, et al. Experimental study and demonstration of pilot-scale, dry feed, oxy-coal combustion under pressure. Applied Energy. 2021;285:116367.
[27] Gopan A, Kumfer BM, Phillips J, Thimsen D, Smith R, Axelbaum RL. Process design and performance analysis of a Staged, Pressurized Oxy-Combustion (SPOC) power plant for carbon capture. Applied Energy. 2014;125:179-88.
[28] Gopan A, Kumfer BM, Axelbaum RL. Effect of operating pressure and fuel moisture on net plant efficiency of a staged, pressurized oxy-combustion power plant. International Journal of Greenhouse Gas Control. 2015;39:390-6.
[29] Xia F, Yang Z, Adeosun A, Gopan A, Kumfer BM, Axelbaum RL. Pressurized oxy-combustion with low flue gas recycle: Computational fluid dynamic simulations of radiant boilers. Fuel. 2016;181:1170-8.
[30] Darde A, Prabhakar R, Tranier J-P, Perrin N. Air separation and flue gas compression and purification units for oxy-coal combustion systems. Energy Procedia. 2009;1:527-34.
[31] Duan Y, Duan L, Anthony EJ, Zhao C. Nitrogen and sulfur conversion during pressurized pyrolysis under CO2 atmosphere in fluidized bed. Fuel. 2017;189:98-106.
[32] Gazzino M, Benelli G. Pressurised Oxy-Coal Combustion Rankine-Cycle for Future Zero Emission Power Plants: Process Design and Energy Analysis. ASME 2008 2nd International Conference on Energy Sustainability collocated with the Heat Transfer, Fluids Engineering, and 3rd Energy Nanotechnology Conferences2008. p. 269-78.
[33] Gazzino M, Riccio G, Rossi N, Benelli G. Pressurised Oxy-Coal Combustion Rankine-Cycle for Future Zero Emission Power Plants: Technological Issues. Asme International Conference on Energy Sustainability Collocated with the Heat Transfer & Interpack09 Conferences2009.
[34] Malavasi M, Rossetti E. High-efficiency combustors with reduced environmental impact and processes for power generation derivable therefrom. WO; 2013.
[35] Hong J, Chaudhry G, Brisson JG, Field RP, Gazzino M, Ghoniem AF. Analysis of oxy-fuel combustion power cycle utilizing a pressurized coal combustor. Energy. 2009;34:1332-40.
[36] Zebian H, Rossi N, Gazzino M, Cumbo D, Mitsos A. Optimal design and operation of pressurized oxy-coal combustion with a direct contact separation column. Energy. 2013;49:268-78.
[37] Hagi H, Nemer M, Le Moullec Y, Bouallou C. Towards second generation oxy-pulverized coal power plants: energy penalty reduction potential of pressurized oxy-combustion systems. Energy Procedia. 2014;63:431-9.

[38] Zebian H, Mitsos A. Pressurized oxy-coal combustion: Ideally flexible to uncertainties. Energy. 2013;57:513-26.

[39] Axelbaum R, Kumfer B, Gopan A, Yang Z, Phillips J, Pint B. Staged, High-Pressure Oxy-Combustion Technology: Development and Scale-Up. Washington Univ., St. Louis, MO (United States); 2017.

[40] Gopan A, Verma P, Yang Z, Axelbaum RL. Quantitative analysis of the impact of flue gas recirculation on the efficiency of oxy-coal power plants. International Journal of Greenhouse Gas Control. 2020;95:102936.

[41] Châtel-Pélage F, Varagani R, Pranda P, Perrin N, Bose A. Applications of Oxygen for NOx Control and CO 2 Capture in Coal-Fired Power Plants. Thermal Science. 2006;10:119-42.

[42] Miller JA, Bowman CT. Mechanism and modeling of nitrogen chemistry in combustion. Progress in energy and combustion science. 1989;15:287-338.

[43] Zeldvich YB. The oxidation of nitrogen in combustion and explosions. J Acta Physicochimica. 1946;21:577.

[44] Glarborg P, Miller JA, Kee RJ. Kinetic modeling and sensitivity analysis of nitrogen oxide formation in well-stirred reactors. Combustion & Flame. 1986;65:177-202.

[45] Moskaleva L, Lin M-C. The spin-conserved reaction $CH+N_2 \rightarrow H+NCN$: A major pathway to prompt NO studied by quantum/statistical theory calculations and kinetic modeling of rate constant. Proceedings of the Combustion Institute. 2000;28:2393-401.

[46] Phong-Anant D, Wibberley L, Wall T. Nitrogen oxide formation from Australian coals. Combustion and flame. 1985;62:21-30.

[47] Nichols KM, Hedman PO, Smoot LD. Release and reaction of fuel-nitrogen in a high-pressure entrained-coal gasifier. Fuel. 1987;66:1257-63.

[48] Zhou H, Huang Y, Mo G, Liao Z, Cen K. Experimental investigations of the conversion of fuel-N, volatile-N and char-N to NOx and N2O during single coal particle fluidized bed combustion. Journal of the Energy Institute. 2015:S1743967115300520.

[49] Winter F. Formation and Reduction of Pollutants in CFBC: From Heavy Metals, Particulates, Alkali, NOx, N2O, SOx, HCl. Berlin, Heidelberg: Springer Berlin Heidelberg; 2010. p. 43-8.

[50] Duan L, Zhao C, Ren Q, Wu Z, Chen X. NOx precursors evolution during coal heating process in CO2 atmosphere. Fuel. 2011;90:1668-73.

[51] Li YH, Lu GQ, Rudolph V. The kinetics of NO and N_2O reduction over coal chars in fluidised-bed combustion. Chemical Engineering Science. 1998;53:1-26.

[52] Zhou H, Li Y, Li N, Qiu R, Cen K. Conversions of fuel-N to NO and N_2O during devolatilization and char combustion stages of a single coal particle under oxy-fuel fluidized bed conditions. Journal of the Energy Institute. 2018:S174396711730541X.

[53] Perrone D, Castiglione T, Morrone P, Barbarelli S, Amelio M. NOx emissions for oxy-mild combustion of pulverized coal in high temperature pre-heated oxygen. Energy Procedia. 2018;148:567-74.
[54] Leppaelahti J, Koljonen T. Review Nitrogen evolution from coal, peat and wood during gasification: Literature review. Fuel Processing Technology. 1995;43:p.1-45.
[55] Glarborg P, Jensen A, Johnsson JE. Fuel nitrogen conversion in solid fuel fired systems. Progress in energy and combustion science. 2003;29:89-113.
[56] Loffler G, Andahazy D, Wartha C, Winter F, Hofbauer H. NOx and N_2O formation mechanisms - A detailed chemical kinetic modeling study on a single fuel particle in a laboratory-scale fluidized bed. 16th International Conference on Fluidized Bed Combustion2001.
[57] Aho M, Paakkinen K, Pirkonen P, Kilpinen P, Hupa M. The effects of pressure, oxygen partial pressure, and temperature on the formation of N_2O, NO, and NO_2 from pulverized coal. Combustion and Flame. 1995;102:387-400.
[58] Croiset E, Heurtebise C, Rouan J-P, Richard J-R. Influence of pressure on the heterogeneous formation and destruction of nitrogen oxides during char combustion. Combustion and flame. 1998;112:33-44.
[59] Tomeczek J, Gil S. Influence of pressure on the rate of nitric oxide reduction by char. Combustion and Flame. 2001;126:1602-6.
[60] Lasek JA, Janusz M, Zuwała J, Głód K, Iluk A. Oxy-fuel combustion of selected solid fuels under atmospheric and elevated pressures. Energy. 2013;62:105-12.
[61] Aho MJ, Pirkonen PM. Effects of pressure, gas temperature and CO_2 and O_2 partial pressures on the conversion of coal-nitrogen to NO, N2O and NO2. Fuel. 1995;74:1677-81.
[62] Hämäläinen JP, Aho MJ. Conversion of fuel nitrogen through HCN and NH_3 to nitrogen oxides at elevated pressure. Fuel. 1996;75:1377-86.
[63] Gong Z, Shao Y, Pang L, Zhong W, Chen C. Study on the emission characteristics of nitrogen oxides with coal combustion in pressurized fluidized bed. Chinese Journal of Chemical Engineering. 2019;27:1177-83.
[64] Jensen A, Johnsson JE, Andries J, Laughlin K, Read G, Mayer M, et al. Formation and reduction of NOx in pressurized fluidized bed combustion of coal. Fuel. 1995;74:1555-69.
[65] Gil S. Fuel-N conversion to NO, N_2O and N_2 during coal combustion. Fossil Fuel and the Environment. 2012:37.
[66] Svoboda K, Pohořelý M. Influence of operating conditions and coal properties on NOx and N_2O emissions in pressurized fluidized bed combustion of subbituminous coals. Fuel. 2004;83:1095-103.
[67] Lu Y, Jahkola A, Hippinen I, Jalovaara J. The emissions and control of NOx and N_2O in pressurized fluidized bed combustion. Fuel. 1992;71:693-9.
[68] Lu Y. Laboratory studies on devolatilization and char oxidation under PFBC conditions. 2. Fuel nitrogen conversion to nitrogen oxides. Energy & fuels. 1996;10:357-63.

[69] Mallet C, Aho M, Hämäläinen J, Rouan J, Richard J-R. Formation of NO, NO_2, and N_2O from Gardanne lignite and its char under pressurized conditions. Energy & fuels. 1997;11:792-800.
[70] Pang L, Shao Y, Zhong W, Gong Z, Liu H. Experimental study of NOx emissions in a 30 kWth pressurized oxy-coal fluidized bed combustor. Energy. 2020;194:116756.
[71] Hong D, Guo X, Wang C. A reactive molecular dynamics study of HCN oxidation during pressurized oxy-fuel combustion. Fuel Processing Technology. 2021;224:107020.
[72] Liang X, Wang Q, Luo Z, Zhang H, Li K, Feng Y, et al. Simulation of nitrogen transformation in pressurized oxy-fuel combustion of pulverized coal. RSC advances. 2018;8:35690-9.
[73] Okazaki K, Ando T. NOx reduction mechanism in coal combustion with recycled CO_2. Energy. 1997;22:207-15.
[74] Lasek JA, Głód K, Janusz M, Kazalski K, Zuwała J. Pressurized oxy-fuel combustion: A Study of selected parameters. Energy & fuels. 2012;26:6492-500.
[75] Hu Y, Kobayashi N, Hasatani M. Effects of coal properties on recycled-NOx reduction in coal combustion with O2/recycled flue gas. Energy conversion and management. 2003;44:2331-40.
[76] Zan H, Chen X, Ma J, Liu D, Wu Y. Experimental Study of NO (x) Formation in a High-Steam Atmosphere During a Pressurized Oxygen-Fuel Combustion Process. ACS Omega. 2020;5:16037-44.
[77] Winter F, Wartha C, Löffler G, Hofbauer H. The NO and N_2O formation mechanism during devolatilization and char combustion under fluidized-bed conditions. Symposium (international) on combustion: Elsevier; 1996. p. 3325-34.
[78] Winter F, Löffler G, Wartha C, Hofbauer H, Preto F, Anthony EJ. The NO and N_2O formation mechanism under circulating fluidized bed combustor conditions: From the single particle to the pilot‐scale. The Canadian Journal of Chemical Engineering. 1999;77:275-83.
[79] Duan Y, Duan L, Wang J, Anthony EJ. Observation of simultaneously low CO, NOx and SO_2 emission during oxy-coal combustion in a pressurized fluidized bed. Fuel. 2019;242:374-81.
[80] Roy B, Chen L, Bhattacharya S. Nitrogen oxides, sulfur trioxide, and mercury emissions during oxy-fuel fluidized bed combustion of Victorian brown coal. Environmental science & technology. 2014;48:14844-50.
[81] Hayhurst A, Lawrence A. The amounts of NOx and N_2O formed in a fluidized bed combustor during the burning of coal volatiles and also of char. Combustion and flame. 1996;105:341-57.
[82] Ting T, Stanger R, Wall T. Laboratory investigation of high pressure NO oxidation to NO_2 and capture with liquid and gaseous water under oxy-fuel CO2 compression conditions. International Journal of Greenhouse Gas Control. 2013;18:15-22.
[83] Lei M, Huang X, Wang C, Yan W, Wang S. Investigation on SO_2, NO and NO_2 release characteristics of Datong bituminous coal during pressurized oxy-fuel combustion. Journal of Thermal Analysis and Calorimetry. 2016;126:1067-75.

[84] Lin S, Suzuki Y, Hatano H. Effect of Pressure on NOx Emission from Char Particle Combustion. Energy & fuels. 2002;16:634-9.
[85] Veras CAG, Saastamoinen J, De Carvalho Jr JA. Effect of particle size and pressure on the conversion of fuel N to no in the boundary layer during devolatilization stage of combustion. Symposium (International) on Combustion: Elsevier; 1998. p. 3019-25.
[86] Gil S. Influence of combustion pressure on fuel-N conversion to NO, N_2O and N_2. Karbo. 2002:272-5.
[87] Solomon PR, Fletcher TH. Impact of coal pyrolysis on combustion. Symposium (International) on Combustion: Elsevier; 1994. p. 463-74.
[88] Cai H-Y, Güell A, Dugwell D, Kandiyoti R. Heteroatom distribution in pyrolysis products as a function of heating rate and pressure. Fuel. 1993;72:321-7.
[89] Niksa S, Liu G-S, Hurt RH. Coal conversion submodels for design applications at elevated pressures. Part I. devolatilization and char oxidation. Progress in Energy and Combustion Science. 2003;29:425-77.
[90] Megaritis A, Messenböck R, Collot A-G, Zhuo Y, Dugwell D, Kandiyoti R. Internal consistency of coal gasification reactivities determined in bench-scale reactors: effect of pyrolysis conditions on char reactivities under high-pressure CO2. Fuel. 1998;77:1411-20.
[91] Lee CW, Scaroni AW, Jenkins RG. Effect of pressure on the devolatilization and swelling behaviour of a softening coal during rapid heating. Fuel. 1991;70:957-65.
[92] Johnsson JE. Formation and reduction of nitrogen oxides in fluidized-bed combustion. Fuel. 1994;73:1398-415.
[93] Li C-Z, Tan LL. Formation of NOx and SOx precursors during the pyrolysis of coal and biomass. Part III. Further discussion on the formation of HCN and NH3 during pyrolysis. Fuel. 2000;79:1899-906.
[94] Gibbins JR, Gonenc ZS, Kandiyoti R. Pyrolysis and hydropyrolysis of coal: comparison of product distributions from a wire-mesh and a hot-rod reactor. Fuel. 1991;70:621-6.
[95] Bautista JR, Russel WB, Saville DA. Time-resolved pyrolysis product distributions of softening coals. Industrial & engineering chemistry fundamentals. 1986;25:536-44.
[96] Tian F-J, Wu H, Yu J-l, McKenzie LJ, Konstantinidis S, Hayashi J-i, et al. Formation of NOx precursors during the pyrolysis of coal and biomass. Part VIII. Effects of pressure on the formation of NH_3 and HCN during the pyrolysis and gasification of Victorian brown coal in steam. Fuel. 2005;84:2102-8.
[97] Sathe C, Hayashi J-I, Li C-Z. Release of volatiles from the pyrolysis of a Victorian lignite at elevated pressures. Fuel. 2002;81:1171-8.
[98] Tan LL, Li C-Z. Formation of NOx and SOx precursors during the pyrolysis of coal and biomass. Part I. Effects of reactor configuration on the determined yields of HCN and NH_3 during pyrolysis. Fuel. 2000;79:1883-9.

[99] Tan LL, Li C-Z. Formation of NOx and SOx precursors during the pyrolysis of coal and biomass. Part II. Effects of experimental conditions on the yields of NOx and SOx precursors from the pyrolysis of a Victorian brown coal. Fuel. 2000;79:1891-7.
[100] Li X, Wu H. Hayashi J-i, Li, C-Z. Fuel. 2004;83:1273.
[101] Bayarsaikhan B, Sathe C, Shimada T, Li C, Hayashi J, Chiba T. Pressure effects on kinetics of steam gasification of nascent char formed from the rapid pyrolysis of a Victorian brown coal. 2003.
[102] Laughlin KM, Gavin DG, Reed GP. Coal and char nitrogen chemistry during pressurized fluidized bed combustion. Fuel. 1994;72:696-.
[103] Maliutina, Kristina, Tahmasebi, Arash, Yu, Jianglong. The transformation of nitrogen during pressurized entrained-flow pyrolysis of Chlorella vulgaris. Bioresource Technology Biomass Bioenergy Biowastes Conversion Technologies Biotransformations Production Technologies. 2018.
[104] Hansen S, Glarborg P. A simplified model for volatile-N oxidation. Energy & fuels. 2010;24:2883-90.
[105] Bowman CT. Control of combustion-generated nitrogen oxide emissions: Technology driven by regulation. Symposium on Combustion. 1992;24:859-78.
[106] Glarborg P. Hidden interactions—Trace species governing combustion and emissions. Proceedings of the Combustion Institute. 2007;31:77-98.
[107] Lucassen A, Zhang K, Warkentin J, Moshammer K, Glarborg P, Marshall P, et al. Fuel-nitrogen conversion in the combustion of small amines using dimethylamine and ethylamine as biomass-related model fuels. Combustion and Flame. 2012;159:2254-79.
[108] Murakami N, Tokunaga K, Sakai M. Formation of NO by the Oxidation of HCN. Nenryo Kyokai-Shi/Journal of the Fuel Society of Japan. 1982;61:759-69.
[109] Miller JA, Branch MC, Mclean WJ, Chandler DW, Smooke MD, Kee RJ. The conversion of HCN to NO and N_2 in H_2−O_2−HCN−Ar flames at low pressure. Symposium on Combustion. 1985;20:673-84.
[110] Hulgaard T, Dam-Johansen K. Homogeneous nitrous oxide formation and destruction under combustion conditions. Aiche Journal. 1993.
[111] Glarborg P, Miller JA. Mechanism and modeling of hydrogen cyanide oxidation in a flow reactor. Combustion & Flame. 1994;99:475-83.
[112] PHILIPPE, DAGAUT, FRANCK, LECOMTE, SéBASTIEN, CHEVAILLER, et al. The Oxidation of HCN and Reactions with Nitric Oxide: Experimental and Detailed Kinetic Modeling. Combustion Science & Technology. 2000.
[113] Wargadalam VJ, Löffler G, Winter F, Hofbauer H. Homogeneous formation of NO and N_2O from the oxidation of HCN and NH_3 at 600–1000°C. Combustion and Flame. 2000.
[114] Gimenez-Lopez J, Millera A, Bilbao R, Alzueta MU. HCN oxidation in an O_2/CO_2 atmosphere: An experimental and kinetic modeling study. Combustion & Flame. 2010;157:267-76.

[115] Giménez-López J, Millera Á, Bilbao R, Alzueta MU. Interactions of HCN with NO in a CO_2 Atmosphere Representative of Oxy-fuel Combustion Conditions. Energy & Fuels. 2015.

[116] Glarborg P, Marshall P. Importance of the Hydrogen Isocyanide Isomer in Modeling Hydrogen Cyanide Oxidation in Combustion. Energy & Fuels. 2017;31:2156-63.

[117] Glarborg, Peter, Miller, James, A., Ruscic, et al. Modeling nitrogen chemistry in combustion. Progress in Energy & Combustion Science. 2018.

[118] a SPC, a OM, b IS, a ELP. High-pressure ignition delay time measurements of a four-component gasoline surrogate and its high-level blends with ethanol and methyl acetate. Fuel.275.

[119] Liu Y, Cheng J, Zou C, Lu L, Jing H. Ignition delay times of ethane under O_2/CO_2 atmosphere at different pressures by shock tube and simulation methods. Combustion & Flame. 2019;204:380-90.

[120] Xiao H, Valera-Medina A, Marsh R, Bowen PJ. Numerical study assessing various ammonia/methane reaction models for use under gas turbine conditions. Fuel. 2017;196:344-51.

[121] Xu D, Tree DR, Lewis RS. The effects of syngas impurities on syngas fermentation to liquid fuels. Biomass & Bioenergy. 2011;35:p.2690-6.

[122] Sukumaran S, Kong SC. Modeling fuel NOx formation from combustion of biomass-derived producer gas in a large-scale burner. Combustion & Flame. 2013;160:2159-68.

[123] Salimian S, Hanson RK, Kruger CH. Ammonia oxidation in shock-heated NH_3, N_2O and Ar mixtures. Combustion & Flame. 1984;56:83-95.

[124] Miller JA, Glarborg P. Modeling the thermal De‐NOx process: Closing in on a final solution. International Journal of Chemical Kinetics. 1999;31:757-65.

[125] Schmidt C, Bowman C. Flow reactor study of the effect of pressure on the thermal de-NOx process. Combustion and flame. 2001;127:1958-70.

[126] Miller JA, Pilling MJ, Troe J. Unravelling combustion mechanisms through a quantitative understanding of elementary reactions. Proceedings of the Combustion Institute. 2005;30:43-88.

[127] Duynslaegher C, Jeanmart H, Vandooren J. KINETICS IN AMMONIA-CONTAINING PREMIXED FLAMES AND A PRELIMINARY INVESTIGATION OF THEIR USE AS FUEL IN SPARK IGNITION ENGINES. Combustion Science & Technology. 2009;181:1092-106.

[128] Mathieu O, Petersen EL. Experimental and modeling study on the high-temperature oxidation of Ammonia and related NOx chemistry. Combustion & Flame. 2015;162:554-70.

[129] Dean AM, Hardy JE, Lyon RK. Kinetics and mechanism of NH_3 oxidation. 1982;19:97-105.

[130] Miller JA, Smooke MD, Green RM, Kee RJ. Kinetic Modeling of the Oxidation of Ammonia in Flames. Combustion Science & Technology. 1983;34:149-76.

[131] Lindstedt RP, Lockwood FC, Selim MA. A Detailed Kinetic Study of Ammonia Oxidation. Combustion Science & Technology. 1995;108:231-54.

[132] Dean AM, Bozzelli JW. Combustion Chemistry of Nitrogen: Springer New York; 2000.

[133] Skreiberg O, Kilpinen P, Glarborg P. Ammonia chemistry below 1400 K under fuel-rich conditions in a flow reactor. Combustion & Flame. 2004;136:p.501-18.
[134] Duynslaegher C, Contino F, Vandooren J, Jeanmart H. Modeling of ammonia combustion at low pressure. Combustion & Flame. 2012;159:p.2799-805.
[135] Teresa, Mendiara, and, Peter, Glarborg. Ammonia chemistry in oxy-fuel combustion of methane. Combustion & Flame. 2009.
[136] Song Y, Hashemi H, Christensen JM, Zou C, Marshall P, Glarborg P. Ammonia oxidation at high pressure and intermediate temperatures. Fuel. 2016;181:358-65.
[137] Klippenstein SJ, Harding LB, Glarborg P, Miller JA. The role of NNH in NO formation and control. Combustion and Flame. 2011;158:774-89.
[138] Duynslaegher C, Jeanmart H, Vandooren J. Ammonia combustion at elevated pressure and temperature conditions. Fuel. 2010;89:P.3540-5.
[139] Kasuya F, Glarborg P, Johnsson JE, Dam-Johansen K. The thermal De-NOx process: Influence of partial pressures and temperature. Chemical Engineering Science. 1995;50:1455-66.
[140] Muzio LJ. Gas phase decomposition of nitric oxide in combustion products. Symposium on Combustion. 1977;16:199-208.
[141] Alzueta MU, Bilbao R, Millera A, M. Oliva A, Ibañez JC. Interactions between Nitric Oxide and Urea under Flow Reactor Conditions. Documento estadistico de trabajo no6. 1998;12:672-80.
[142] Lee S, Park K, Park JW, Kim BH. Characteristics of reducing NO using urea and alkaline additives. Combustion & Flame. 2005;141:p.200-3.
[143] Alzueta MU, Bilbao R, Millera A, Oliva M, Iba?ez JC. Impact of New Findings Concerning Urea Thermal Decomposition on the Modeling of the Urea-SNCR Process. Energy & Fuels. 2000;14:509-10.
[144] Perry RA, Siebers DL. Rapid reduction of nitrogen oxides in exhaust gas streams. Nature. 1986;324:657-8.
[145] Glarborg P, Kristensen PG, Jensen SRH, Dam-Johansen K. A flow reactor study of HNCO oxidation chemistry. Combustion & Flame. 1994;98:241-58.
[146] Lyon RK, Cole JA. A Reexamination of the RapreNOx Process. Combustion & Flame. 1990;82:435-43.
[147] Wicke BG, Grady KA, Ratcliffe JW. Cyanuric acid + nitric oxide reaction at 700°C and the effects of oxygen. Combustion & Flame. 1989;78:249-55.
[148] Javed MT, Ahmed Z, Ibrahim MA, Irfan N. A comparative kinetic study of SNCR process using ammonia. Brazilian Journal of Chemical Engineering. 2008;25:109-17.
[149] Zabetta EC, Hupa M, Saviharju K. Reducing NOx emissions using fuel staging, air staging, and selective noncatalytic reduction in synergy. Industrial & engineering chemistry research. 2005;44:4552-61.

[150] ur Rahman Z, Wang X, Zhang J, Baleta J, Vujanović M, Tan H. Kinetic study and optimization on SNCR process in pressurized oxy-combustion. Journal of the Energy Institute. 2020.
[151] Miller JA, Glarborg P. Modelling the formation of N_2O and NO_2 in the thermal De-NO x process. Gas phase chemical reaction systems: Springer; 1996. p. 318-33.
[152] Lyon RK, Hardy JE. Discovery and development of the thermal De-NOx process. Industrial & engineering chemistry fundamentals. 1986;25:19-24.
[153] Miller JA, Branch MC, Kee RJ. A chemical kinetic model for the selective reduction of nitric oxide by ammonia. Combustion and Flame. 1981;43:81-98.
[154] Lu Z-m, Lu J-d. Influences of O2 concentration on NO reduction and N_2O formation in thermal deNOx process. Combustion and flame. 2009;156:1303-15.
[155] Glarborg P, Kubel D, Dam‐Johansen K, Chiang HM, Bozzelli JW. Impact of SO_2 and NO on CO oxidation under post‐flame conditions. International Journal of Chemical Kinetics. 1996;28:773-90.
[156] Mueller M, Yetter RA, Dryer F. Kinetic modeling of the $CO/H_2O/O_2/NO/SO_2$ system: Implications for high‐pressure fall‐off in the SO_2+ O (+M)= SO_3 (+M) reaction. International Journal of Chemical Kinetics. 2000;32:317-39.
[157] ZuR, XW, JZ, JB, MV, HT. Kinetic study and optimization on SNCR process in pressurized oxy-combustion. Journal of the Energy Institute. 2020.
[158] ROTA R, Antos D, Zanoelo E, Carra S. Experimental study and kinetic modelling of nitric oxide reduction with ammonia. Combustion science and technology. 2001;163:25-47.
[159] Dagaut P, Nicolle A. Experimental and kinetic modeling study of the effect of SO_2 on the reduction of NO by ammonia. Proceedings of the Combustion Institute. 2005;30:1211-8.
[160] Yilmaz A, Hindiyarti L, Jensen AD, Glarborg P, Marshall P. Thermal Dissociation of SO_3 at 1000− 1400 K. The Journal of Physical Chemistry A. 2006;110:6654-9.
[161] Dayma G, Dagaut P. Effects of air contamination on the combustion of hydrogen—effect of NO and NO2 addition on hydrogen ignition and oxidation kinetics. Combustion science and technology. 2006;178:1999-2024.
[162] Mueller M, Yetter R, Dryer F. Kinetic modeling of the $CO/H_2O/O_2/NO/SO_2$ system: Implications for high‐pressure fall‐off in the SO_2+ O (+M)= SO_3 (+M) reaction. International Journal of Chemical Kinetics. 2000;32:317-39.
[163] Wang X, Yablonsky GS, ur Rahman Z, Yang Z, Du P, Tan H, et al. Assessment of sulfur trioxide formation due to enhanced interaction of nitrogen oxides and sulfur oxides in pressurized oxy-combustion. Fuel. 2021;290:119964.
[164] Kj K, Glarborg P, Dam-Johansen K, Miller JA. Pressure effects on the thermal de-NOx process. Symposium (International) on Combustion: Elsevier; 1996. p. 2067-74.

[165] Glarborg P, Karll B, Pratapas J. Review of Natural Gas Reburning. Initial Full Scale Results. Nineteenth World Gas Conference1994. p. 20-3.
[166] Chen SL, Kramlich JC, Seeker WR, Pershing DW. Optimization of Reburning for Advanced N0x Control on Coal-fired Boilers. Japca. 1989;39:1375-9.
[167] Dagaut P, Lecomte F. Experiments and kinetic modeling study of NO-reburning by gases from biomass pyrolysis in a JSR. Energy & fuels. 2003;17:608-13.
[168] Dagaut P, Luche J, Cathonnet M. The kinetics of C_1 to C_4 hydrocarbons/NO interactions in relation with reburning. Proceedings of the Combustion Institute. 2000;28:2459.
[169] Pershing DW. Bench and pilot scale process evaluation of reburning for in-furnace NOx reduction. Symposium1986.
[170] Smart JP, Morgan DJ. The effectiveness of multi-fuel reburning in an internally fuel-staged burner for NOx reduction. Fuel. 1994;73:1437-42.
[171] Glarborg P, Alzueta MU, Dam-Johansen K, Miller JA. Kinetic Modeling of Hydrocarbon/Nitric Oxide Interactions in a Flow Reactor. Combustion & Flame. 1998;115:1-27.
[172] Mendiara T, Glarborg P. Reburn chemistry in oxy-fuel combustion of methane. Energy & fuels. 2009;23:3565-72.
[173] Bilbao R, Alzueta MU, Millera A. Experimental Study of the Influence of the Operating Variables on Natural Gas Reburning Efficiency. Fuel & Energy Abstracts. 1995;37:215–33.
[174] Bilbao R, Millera A, Alzueta MU, Prada L. Evaluation of the use of different hydrocarbon fuels for gas reburning. Fuel. 1997;76:1401-7.
[175] Alzueta MU, Glarborg P, Dam-Johansen K. Low temperature interactions between hydrocarbons and nitric oxide: an experimental study. Combustion and flame. 1997;109:25-36.
[176] Myerson AL. The reduction of nitric oxide in simulated combustion effluents by hydrocarbon-oxygen mixtures. Symposium (International) on Combustion: Elsevier; 1975. p. 1085-92.
[177] Giménez-López J, Aranda V, Millera A, Bilbao R, Alzueta M. An experimental parametric study of gas reburning under conditions of interest for oxy-fuel combustion. Fuel processing technology. 2011;92:582-9.
[178] Bartok W, DEL VALLE E. Basic kinetic studies and modeling of nitrogen oxide formation in combustion processes. 1972.
[179] Dagaut P, Lecomte F, Chevailler S, Cathonnet M. Experimental and detailed kinetic modeling of nitric oxide reduction by a natural gas blend in simulated reburning conditions. Combustion Science and Technology. 1998;139:329-63.
[180] Dagaut P, Luche J, Cathonnet M. The kinetics of C_1 to C_4 hydrocarbons/NO interactions in relation with reburning. Proceedings of the Combustion Institute. 2000;28:2459-65.
[181] Kilpinen P, Glarborg P, Hupa M. Reburning chemistry: a kinetic modeling study. Industrial & engineering chemistry research. 1992;31:1477-90.

[182] Ledesma EB, Nelson PF, Mackie JC. An experimental and kinetic modeling study of the reduction of NO by coal volatiles in a flow reactor. Proceedings of the Combustion Institute. 2000;28:2345-51.
[183] Glarborg P, Kristensen PG, Dam-Johansen K, Alzueta MU, Bilbao R, Millera A. Nitric Oxide Reduction by Non-hydrocarbon Fuels-Implications for Reburning with Biomass Fuels. 5th International Conference on Technologies and Combustion for a Clean Environment1999.
[184] Faravelli T, Frassoldati A, Ranzi E. Kinetic modeling of the interactions between NO and hydrocarbons in the oxidation of hydrocarbons at low temperatures. Combustion and Flame. 2003;132:188-207.
[185] Li P, Li W, Wang K, Hu F, Ding C, Guo J, et al. Experiments and kinetic modeling of NO reburning by CH_4 under high CO_2 concentration in a jet-stirred reactor. Fuel. 2020;270:117476.
[186] ur Rahman Z, Zhang J, Zhang L, Wang X, Yang Z, Tan H, et al. A kinetic evaluation and optimization study on NOx reduction by reburning under pressurized oxy-combustion. Journal of Environmental Management. 2021;290:112690.
[187] Gregory P. Smith DMG, Michael Frenklach, Nigel W. Moriarty, Boris Eiteneer, Mikhail Goldenberg, C. Thomas Bowman, Ronald K. Hanson, Soonho Song, William C. Gardiner, Jr., Vitali V. Lissianski, and Zhiwei Qin. GRI-Mech 3.0, <http://www.me.berkeley.edu/gri_mech/>.
[188] C.T. Bowman RKH, D.F. Davidson, W.C. Gardiner, Jr., V. Lissianski, G.P. Smith, D.M. Golden, M. Frenklach and M. Goldenberg,. GRI-Mech 2.11, <http://www.me.berkeley.edu/gri_mech/>.
[189] Konnov AA. Implementation of the NCN pathway of prompt-NO formation in the detailed reaction mechanism. Combustion and Flame. 2009;156:2093-105.
[190] B DLA, B WLA, B QCA, B JJA, B JCA. Measurement and modeling of nitrogen oxides absorption in a pressurized reactor relevant to CO 2 compression and purification process. International Journal of Greenhouse Gas Control.100.
[191] Normann F, Jansson E, Petersson T, Andersson K. Nitrogen and sulphur chemistry in pressurised flue gas systems: A comparison of modelling and experiments. International Journal of Greenhouse Gas Control. 2013;12:26-34.
[192] Morrison ME, Rinker RG, Corcoran WH. Rate and Mechanism of Gas-Phase Oxidation of Parts-Per-Million Concentrations of Nitric Oxide. Industrial & Engineering Chemistry Fundamentals. 1966;5:175-81.
[193] Atkinson R, Baulch DL, Cox RA, Crowley JN, Troe J. Evaluated kinetic and photochemical data for atmospheric chemistry: Volume I - gas phase reactions of ceOx, ceHOx, ceNx and ceSOx species. ATMOSPHERIC CHEMISTRY AND PHYSICS. 2004;4:1461-738.
[194] Mueller M, Yetter R, Dryer F. Flow reactor studies and kinetic modeling of the H_2/O_2/NOx and CO/H2O/O2/NOx reactions. International Journal of Chemical Kinetics. 1999;31:705-24.

[195] Hori M, Matsunaga N, Marinov N, William P, Charles W. An experimental and kinetic calculation of the promotion effect of hydrocarbons on the NO-NO_2 conversion in a flow reactor. Symposium (International) on Combustion: Elsevier; 1998. p. 389-96.
[196] Sano T. NO2 Formation in Laminar Flames. Combustion ence & Technology. 2007;29:261-75.
[197] Hargeaves KJA, Harvey R, Roper FG, Smith DB. Formantion of NO_2 by laminar flames. Symposium on Combustion. 1981;18:133-42.
[198] Hori M. Experimental study of nitrogen dioxide formation in combustion systems. Symposium on Combustion. 1988;21:1181-8.
[199] Wang X, Dai G, Yablonsk GS, Vujanović M, Axelbaum RL. A kinetic evaluation on NO_2 formation in the post-flame region of pressurized oxy-combustion process. Thermal Science. 2020:236-.
[200] Hunderup, J. W, Roby, R. J. An experimental investigation of the conversion of NO to NO_2 at high pressure. Journal of Engineering for Gas Turbines & Power. 1996.
[201] Dayma G, Dagaut P. EFFECTS OF AIR CONTAMINATION ON THE COMBUSTION OF HYDROGEN—EFFECT OF NO AND NO_2 ADDITION ON HYDROGEN IGNITION AND OXIDATION KINETICS. Combustion Science & Technology. 2006;178:1999-2024.
[202] Tumsa, Tefera, Zelalem, Lee, See, Hoon, et al. Concomitant removal of NOx and SOx from a pressurized oxy-fuel combustion process using a direct contact column. Chemical Engineering Research & Design Transactions of the Institution of Chemical Engineers. 2018.
[203] Liémans I, Alban B, Tranier JP, Thomas D. SOx and NOx absorption based removal into acidic conditions for the flue gas treatment in oxy-fuel combustion. Energy Procedia. 2011;4:2847-54.
[204] Tranier J-P, Liquide A. CO_2 purification unit for oxy-coal combustion systems. 1st International Oxyfuel Combustion Conference2009.
[205] Lockwood F, Granados L, Leclerc M, Lesort A-L, Beasse G, Delgado MA, et al. Oxy-combustion CPU–From pilots towards industrial-scale demonstration. Energy Procedia. 2014;63:342-51.
[206] Shah M, Degenstein N, Zanfir M, Kumar R, Bugayong J, Burgers K. Near zero emissions oxy-combustion CO2 purification technology. Energy Procedia. 2011;4:988-95.
[207] Verma P, Gromotka Z, Yablonsky G, Stokie D, Constales D, Kumfer B, et al. Optimizing complexity in the kinetic modelling of integrated flue gas purification for pressurized oxy-combustion. Chemical Engineering Journal. 2020;383:122875.
[208] Axelbaum R, Stokie D, Verma P, Kumfer B, Min Y, Zhu Y, et al. Integrated Flue Gas Purification and Latent Heat Recovery for Pressurized Oxy-Combustion. Washington Univ., St. Louis, MO (United States); 2019.
[209] Ajdari S, Normann F, Andersson K, Johnsson F. Reduced mechanism for nitrogen and sulfur chemistry in pressurized flue gas systems. Industrial & Engineering Chemistry Research. 2016;55:5514-25.

[210] Terraglio FP, Manganelli RM. The absorption of atmospheric sulfur dioxide by water solutions. Journal of the Air Pollution Control Association. 1967;17:403-6.
[211] Tsukahara H, Ishida T, Mayumi M. Gas-phase oxidation of nitric oxide: chemical kinetics and rate constant. Nitric Oxide. 1999;3:191-8.
[212] Torrente-Murciano L, White V, Petrocelli F, Chadwick D. Study of individual reactions of the sour compression process for the purification of oxyfuel-derived CO_2. International Journal of Greenhouse Gas Control. 2011;5:S224-S30.
[213] Cheng Q, Liu D, Chen J, Jin J, Li W, Yu S. Gas-phase oxidation of NO at high pressure relevant to sour gas compression purification process for oxy-fuel combustion flue gas. Chinese Journal of Chemical Engineering. 2019;27:884-95.
[214] Murciano LT, White V, Petrocelli F, Chadwick D. Sour compression process for the removal of SOx and NOx from oxyfuel-derived CO2. Energy Procedia. 2011;4:908-16.
[215] Stanger R, Ting T, Spero C, Wall T. Oxyfuel derived CO_2 compression experiments with NOx, SOx and mercury removal—Experiments involving compression of slip-streams from the Callide Oxyfuel Project (COP). International Journal of Greenhouse Gas Control. 2015;41:50-9.
[216] Chang S, Littlejohn D, Lin N. Kinetics of reactions in a wet flue gas simultaneous desulfurization and denitrification system. ACS Publications; 1982.
[217] Oblath S, Markowitz S, Novakov T, Chang S. Kinetics of the formation of hydroxylamine disulfonate by reaction of nitrite with sulfites. The Journal of Physical Chemistry. 1981;85:1017-21.
[218] Oblath S, Markowitz S, Novakov T, Chang S. Kinetics of the initial reaction of nitrite ion in bisulfite solutions. The Journal of Physical Chemistry. 1982;86:4853-7.
[219] Susianto, Petrissans M, Zoulalian A. Influence of the pH on the interactions between nitrite and sulfite ions. Kinetic of the reaction at pH4 and 5. Industrial & engineering chemistry research. 2001;40:6068-72.
[220] De Soete G. Heterogeneous N2O and NO formation from bound nitrogen atoms during coal char combustion. Symposium (International) on Combustion: Elsevier; 1991. p. 1257-64.
[221] Rodriguez-Mirasol J, Ooms A, Pels J, Kapteijn F, Moulijn J. NO and N_2O decomposition over coal char at fluidized-bed combustion conditions. Combustion and Flame. 1994;99:499-507.
[222] Zhang J, Chen C, Zhou A, ur Rahman Z, Wang X, Stojiljković D, et al. Morphology of char particles from coal pyrolysis in a pressurized entrained flow reactor: Effects of pressure and atmosphere. Energy. 2022;238:121846.

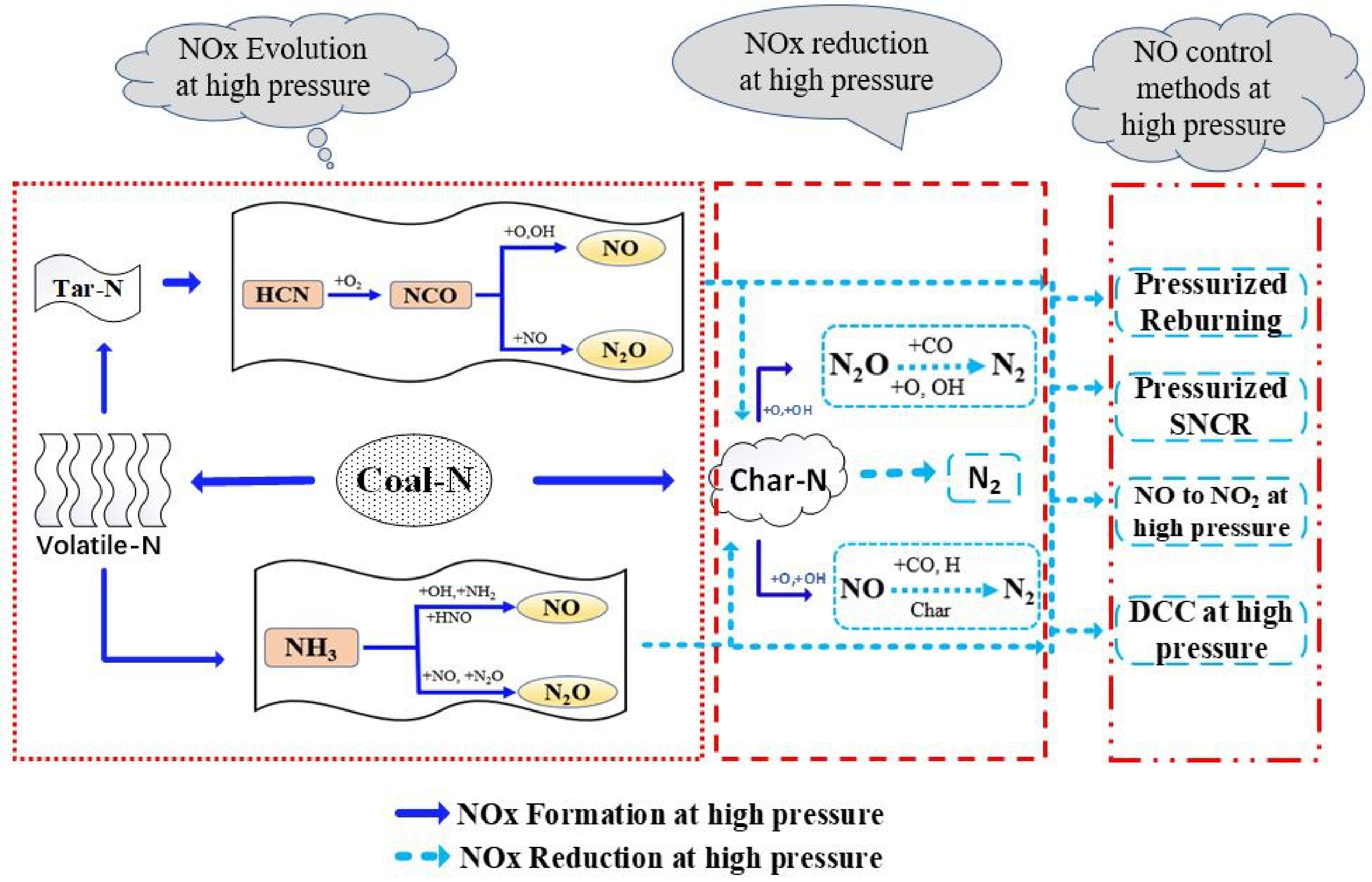

NOx Evolution at high pressure
NOx reduction at high pressure
NO control methods at high pressure
Tar-N
HCN
+O₂
NCO
+O,OH
NO
+NO
N₂O
Volatile-N
Coal-N
NH₃
+OH,+NH₂
+HNO
NO
+NO, +N₂O
N₂O
Char-N
+O,+OH
N₂O
+CO
+O, OH
N₂
N₂
+O,+OH
NO
+CO, H
Char
N₂
Pressurized Reburning
Pressurized SNCR
NO to NO₂ at high pressure
DCC at high pressure
NOx Formation at high pressure
NOx Reduction at high pressure